Palaeogeography, Palaeoclimatology, Palaeoecology 694 (2026) 113824

Contents lists available at ScienceDirect

Palaeogeography, Palaeoclimatology, Palaeoecology

journal homepage: www.elsevier.com/locate/palaeo

Review Article

The palynology of the Upper Triassic-Lower Jurassic in the Algarve and Lusitanian basins, Portugal

Margarida Vilas-Boas [a,*], Simonetta Cirilli [a], Zélia Pereira [b], Luís Vítor Duarte [c], Paulo Fernandes [d]

[a] Dipartimento di Fisica e Geologia, Università degli Studi di Perugia, 06123 Perugia, Italy
[b] LNEG, Laboratório Nacional de Energia e Geologia (Geological Survey), Rua da Amieira, 4465-965 S. Mamede de Infesta, Portugal
[c] University of Coimbra, Earth Sciences Department, and Marine and Environmental Sciences Centre (MARE)/ARNET, 3030-790 Coimbra, Portugal
[d] CIMA, Centre of Marine and Environmental Research\ARNET - Infrastructure Network in Aquatic Research, University of Algarve, Campus de Gambelas, 8000-139 Faro, Portugal

ARTICLE INFO

Editor: L Angiolini

Keywords:
Palynostratigraphy
Palaeogeography
Palaeoclimate
Palaeoenvironment
Silves Group
Triassic-Jurassic Boundary

ABSTRACT

High-resolution palynological analyses from the Algarve and Lusitanian basins (Portugal) provide a refined biostratigraphical framework and palaeoenvironmental reconstruction for the Late Triassic–Early Jurassic transition. In the Algarve Basin, three new palynozones (AT, SC, and CP) characterise the Silves Group from the early Carnian to early Hettangian, documenting the first Iberian occurrence of *Tulesporites briscoensis* and precisely delineating the Triassic–Jurassic Boundary (TJB). In the Lusitanian Basin, three palynozones (CG, IK, and Pm) constrain the Conraria and Pereiros formations to the Norian–Hettangian, with the TJB located at the base of the Pereiros Formation. Palaeoenvironmental reconstructions reveal distinct basin-specific evolutions. The Algarve Basin records an early transition from fluvial (Silves Sandstones) to marginal-marine (lagoonal and pond) settings, evidenced by abundant upper Carnian algal elements and reworked Neoproterozoic algae. Conversely, the Lusitanian Basin reflects a Norian-Hettangian marginal-marine, river-dominated setting, with microforaminiferal linings at the base of the Pereiros Formation marking the earliest marine transgression in the Lusitanian Basin. Quantitatively, both basins show a persistent dominance of xerophytic taxa, indicating a shift toward warmer, seasonally dry conditions across the TJB. Malformed sporomorphs in both records suggest environmental stress potentially linked to Central Atlantic Magmatic Province (CAMP) activity. Comparative analysis reveals that sedimentation initiated earlier in the Algarve (early Carnian) than in the Lusitanian Basin (Norian), suggesting diachronous development during Pangaea breakup. The assemblages show strong affinities with the Onslow Microflora, highlighting the Portuguese margin as a key archive for western Tethyan floral and climatic evolution.

1. Introduction

The Triassic-Jurassic Boundary (TJB; 201.4 ± 0.2 Ma; Gradstein and Ogg, 2020) marks one of the most critical intervals in Earth's history, characterized by profound tectonic, climatic and biotic changes. This transition is associated with: (1) the beginning of the Pangaea breakup (Müller et al., 2016); (2) widespread deposition of huge evaporites across continental platforms (e.g. Iberian Peninsula, North of Africa (Buratti and Cirilli, 2007)); (3) a globally warm climate, with the Late Triassic and Early Jurassic considered among the warmest intervals in the Phanerozoic (Vaughan, 2007); (4) deposition of red beds (Cirilli, 2010) and, (5) absence of glacial deposits even at the high palaeolatitudes (Hochuli and Vigran, 2010). This time interval also coincides with the end-Triassic Mass Extinction (ETME), one of the most severe biotic crises recognised in the Phanerozoic (Raup and Sepkoski, 1982; Sepkoski, 1996; Marzoli et al., 2004; Tanner et al., 2004; Nomade et al., 2007; Davies et al., 2017).

This event triggered substantial ecological turnover in both marine and terrestrial realms, with notable extinctions among marine taxa and significant changes in continental flora and fauna (Guex et al., 2004;

* Corresponding author at: Dipartimento di Fisica e Geologia, Università degli Studi di Perugia, 06123 Perugia, Italy.
E-mail addresses: margarida.vboas@gmail.com (M. Vilas-Boas), simonetta.cirilli@unipg.it (S. Cirilli), zelia.pereira@lneg.pt (Z. Pereira), lduarte@dct.uc.pt (L.V. Duarte), pfernandes@ualg.pt (P. Fernandes).

https://doi.org/10.1016/j.palaeo.2026.113824
Received 9 December 2025; Received in revised form 14 April 2026; Accepted 18 April 2026
Available online 21 April 2026

Whiteside et al., 2007; Van de Schootbrugge et al., 2008; Bonis et al., 2010; Lindström, 2016; Lindström et al., 2017a, 2017b, 2021). However, the magnitude of the impact on terrestrial vegetation remains a matter of debate (Tanner et al., 2004; Cirilli et al., 2009; Cirilli, 2010; Lucas et al., 2011). This event is marked by abrupt widespread disruptions in palaeoenvironments and palaeoecosystems, with taxonomic losses estimated to be between 40% and 73%, ranking it as the most severe biotic crisis in Earth's history (Lindström et al., 2017b). Nevertheless, some palynological and macrofloristical data from Europe suggest that the floristic turnover across the TJB may have been more gradual or regionally variable, with no clear evidence of a major extinction (Barbacka et al., 2017).

Furthermore, the TJB is characterized by a significant eustatic regression and a global increase in the relative abundance of spores (Hallam and Wignall, 1999; Hesselbo et al., 2004; Hillebrandt et al., 2013; Lindström et al., 2017a, 2017b; Haq, 2018).

Multiple causes have been proposed to explain this biotic crisis, among which the magmatic activity associated with the Central Atlantic Magmatic Province (CAMP) is widely recognised as a key driver (Marzoli et al., 2004; Nomade et al., 2007; Cirilli et al., 2009; Davies et al., 2017). CAMP magmatism, a prominent marker of the end-Triassic in several regions (e.g., Portugal, North Africa and Eastern North America), is believed to have led to significant atmospheric emissions of CO_2 and SO_2, which likely intensified the greenhouse effect, triggering a cascade of secondary environmental disturbances, including acid rain, freshwater and marine systems acidification, and a pronounced global warming (Hesselbo et al., 2002; Guex et al., 2004; Marzoli et al., 2004; Tanner et al., 2004, 2007; Nomade et al., 2007; Schaltegger et al., 2008; Van de Schootbrugge et al., 2008, 2009; Cirilli et al., 2009, 2015, 2018; Deenen et al., 2010; Lindström, 2016; Davies et al., 2017; Lindström et al., 2019; Panfili et al., 2019; Capriolo et al., 2020; Trudgill et al., 2025).

The precise timing of CAMP volcanism relative to the TJB has been debated for a long time, with conflicting evidence suggesting that eruptions may have occurred before (Marzoli et al., 1999, 2004, 2008), during, or shortly after the transition (Whiteside et al., 2007).

Nevertheless, several geochronological and biostratigraphical dating documents the synchronicity between the events and support the onset of CAMP activity before the TJB, thereby reinforcing the hypothesis that magmatism played a significant role in triggering the biotic crisis (Marzoli et al., 2008, 2011, 2018; Cirilli et al., 2009; Cirilli, 2010; Blackburn et al., 2013; Dal Corso et al., 2014; Black et al., 2021; Capriolo et al., 2021).

In Portugal, the CAMP is represented by the Messejana Dyke (intrusive body, ~200 Ma; Wilson et al., 1998) and the Volcano–Sedimentary Complex in the Algarve Basin (Verati et al., 2007; Martins et al., 2008). In contrast, the Lusitanian Basin lacks clear evidence of CAMP activity, except in its southernmost sector (Azerêdo et al., 2003; Kullberg et al., 2013).

Additional factors contributing to environmental instability at the TJB include enhanced tectonic activity and significant sea level fluctuations, which are reflected in several sedimentary hiatuses across Western European basins (Lindström et al., 2017a, 2017b; Schneebeli-Hermann et al., 2018). Despite regional differences, these basins commonly exhibit comparable stratigraphical architectures, characterized by a basal continental, sand-rich unit overlain by a finer-grained and mud-prone unit deposited in lacustrine to marginal marine environments (Frizon de Lamotte et al., 2015).

In Portugal, the sedimentary successions from the Triassic to the Lower Jurassic are part of the Silves Group, a stratigraphical unit exposed in the Algarve Basin in the south and in the Lusitanian Basin along the central area (e.g., Palain, 1976; Soares et al., 2012; Kullberg et al., 2013; among others; Figs. 1 and 2). At the end of the Triassic and the beginning of the Jurassic, the margins of the Variscan Iberian Massif were affected by extensional regimes associated with the initial rifting of Pangaea and the early stages of Atlantic Ocean opening (Kullberg et al., 2013).

Although the TJB within the Silves Group in Portugal is still under investigation, palynostratigraphical studies have documented significant changes in palynofloral assemblages across this critical interval (Doubinger et al., 1970; Adloff et al., 1974; Díez, 2000; Arche and López-Gómez, 2014; Vilas-Boas et al., 2021, 2022, 2023, 2024). Present palynological records provide new insights into the dynamics of the end-Triassic biotic crisis and the subsequent recovery during the Early Jurassic, challenging conventional models of ecological resilience and turnover in continental environments. Nonetheless, several stratigraphical and palaeoenvironmental aspects of the Silves Group remain poorly constrained. These include the precise age of the end-Triassic extinction horizon, the extent and timing of CAMP-related environmental perturbations, the nature of sedimentary environments, and the prevailing climatic conditions across the TJB. Establishing a detailed and robust biostratigraphical framework for the Silves Group is therefore essential to fully unravel its stratigraphical record, which may preserve key evidence of profound global change during the Late Triassic to Early Jurassic transition.

The present study contributes to this broader objective by presenting new palynological assemblages from the units of the Silves Group in both Portuguese basins, providing refined age constraints and insights into the palaeoecological evolution of these basins across this critical interval in Earth's history.

2. Geological setting

2.1. Algarve Basin

The Algarve Basin is a Mesozoic-Cenozoic sedimentary basin that unconformably overlies the South Portuguese Zone, which is composed of deep-marine Pennsylvanian strata deformed and metamorphosed during the Variscan Orogeny (Palain, 1976; Terrinha et al., 2013; Figs. 1 and 2). Onshore, the basin extends from Cap São Vicente to the Portuguese-Spanish border. The Mesozoic sedimentary record, linked with the opening of the Atlantic Ocean, reflects a passive margin setting developed throughout multiple extensional phases, from the Late Triassic to the mid-Cretaceous, associated with lithospheric stretching and thinning and the formation of oceanic crust in the western Tethys realm, between the Algarve region and North Africa (Manuppella et al., 1988; Terrinha et al., 2013).

Sedimentation in the Algarve Basin began during the Late Triassic, with the deposition of continental red beds and evaporites, unconformably overlaid by folded and faulted Carboniferous strata (Palain, 1976). Notably, thick evaporitic deposits are restricted to areas south of the *E*-W trending Algibre Fault, whereas they are absent to the north of this important tectonic structure. Volcanic rocks associated with the CAMP overlie these sedimentary units (Verati et al., 2007; Martins et al., 2008).

In the Algarve Basin, geochronological data based on $^{40}Ar/^{39}Ar$ of volcanics located approximately 50 m below the CAMP volcanic interval shows that 198.1 ± 0.4 Ma represents the best estimate of the age of the CAMP volcanism in Portugal (Verati et al., 2007). This chronology is broadly consistent with the late Hettangian age inferred from microfloral assemblages within the overlying evaporites (Fechner, 1989).

The Triassic deposits of the Algarve Basin record a transition from predominantly continental fluvial environments to shallow brackish settings. They include synsedimentary volcanic flows and evaporites, whose precise temporal boundaries remain difficult to establish. The relative chronology of these sedimentary units is poorly constrained due to the lack of age-diagnostic index fossils. Nevertheless, the presence of *Eustheria* sp. (Palain, 1976), vertebrate remains of *Phytosauria* (Mateus et al., 2014) and *Metoposaurus algarvensis* (Brusatte et al., 2015), found above the basal red sandstones, supports a Late Triassic age for this part of the Silves Group succession.

The Silves Group, in the Algarve Basin, represents the earliest

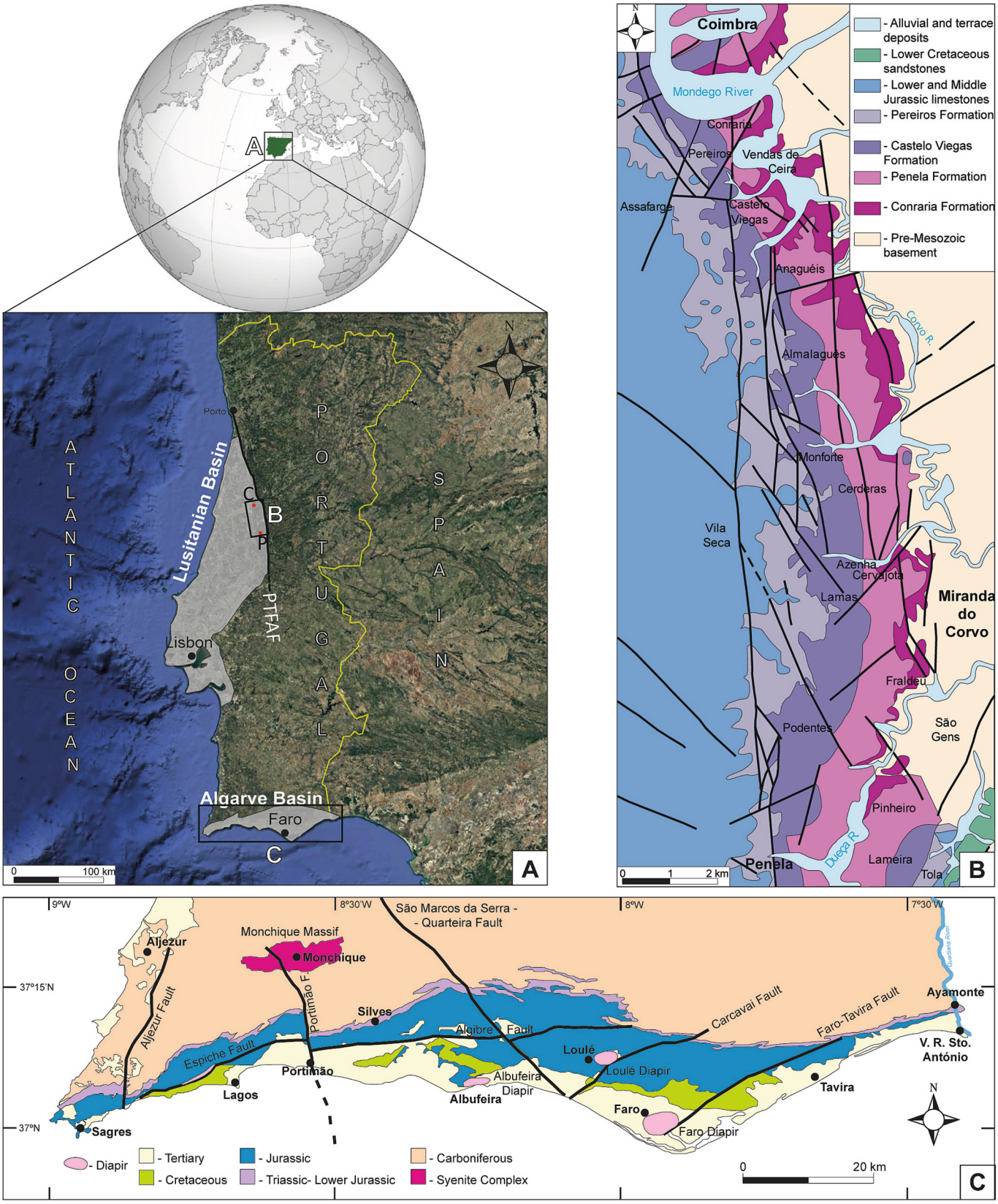

Fig. 1. A - Map of Portugal with the rectangles highlighting the studied areas of the Silves Group in the Lusitanian Basin (B) and Algarve Basin (C). C – Coimbra. P – Penela. PTFAF – Porto-Tomar- Ferreira do Alentejo Fault; B - Map of the studied area in Lusitanian Basin with location of studied sections (based on Soares et al., 2012). Corvo R. – Corvo River. Dueça R. – Dueça River; C - Detailed geological map of the Algarve Basin (based on Oliveira et al., 1992). Portimão F. – Portimão Fault. V. R. Sto. António – Vila Real de Santo António.

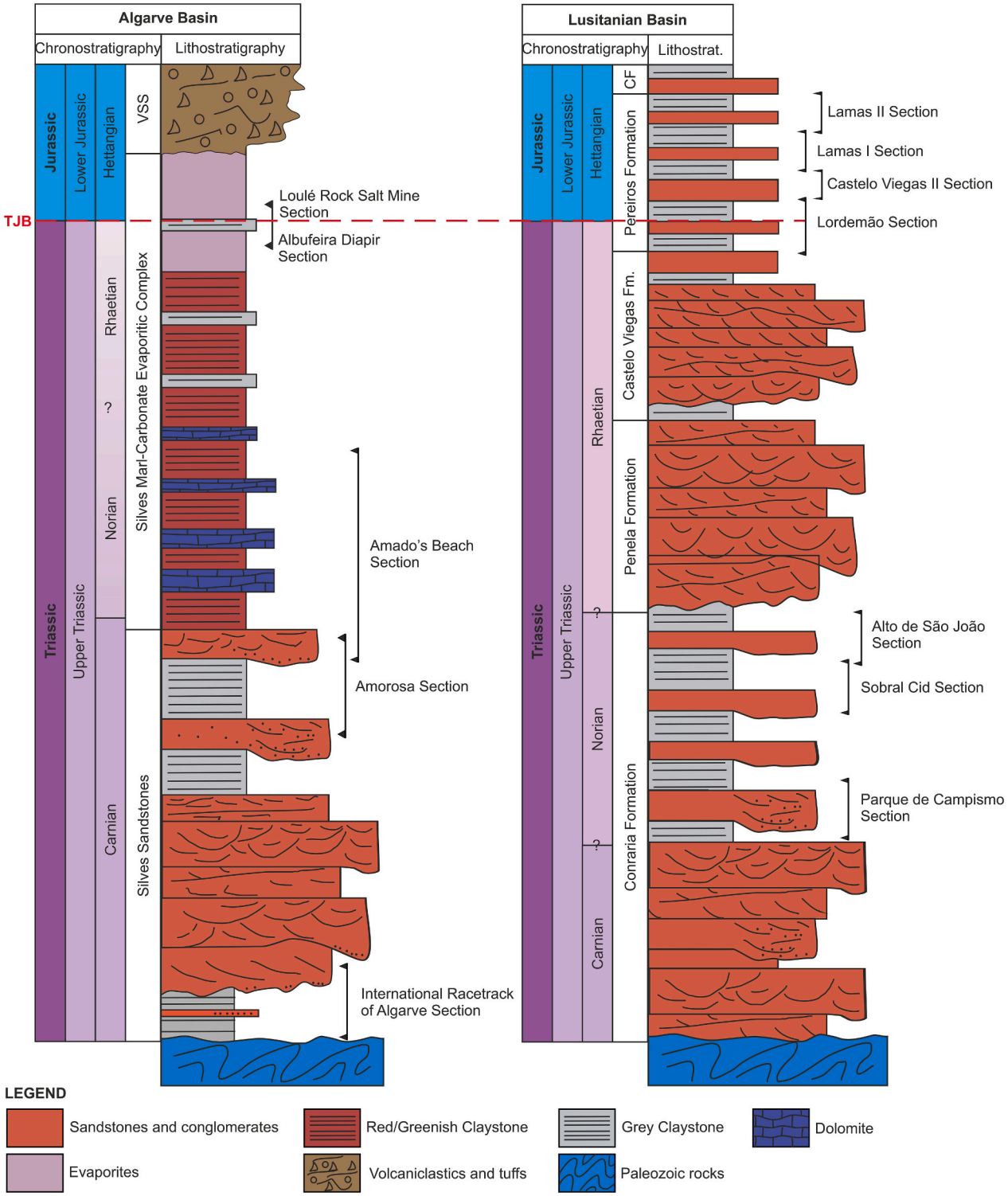

Fig. 2. General stratigraphic log of the Silves Group of the Algarve and Lusitanian (adapted from Soares et al., 2012) basins, with the location of the studied sections of each. TJB – Triassic–Jurassic Boundary. VSS – Volcano–Sedimentary Series. CF – Coimbra Formation. Fm. – Formation. Lithostrat. – Lithostratigraphy.

sedimentary phase, linked to the initial stages of the Pangaea continental rifting. From oldest to youngest, it comprises the following units: São Bartolomeu de Messines Clays, Silves Sandstones, Silves Marl–Carbonate Evaporitic Complex and Volcano–Sedimentary Series (Terrinha et al., 2013; Fig. 3). The Volcano–Sedimentary Series that caps the Silves Group consists mainly of mafic volcanic rocks associated with the CAMP (Martins et al., 2008). The sedimentary facies, textures, and thicknesses of the Silves Sandstones vary across the basin, reflecting lateral changes in depositional setting controlled by their position within the basin (Palain, 1976). A more detailed description of the units of the Silves Group in the Algarve Basin is presented in Supplementary Material A.

The **Silves Sandstones** unit corresponds to the lower part of the Silves Group. It mostly comprises conglomeratic sandstones and red pelites at the base, transitioning upward into red sandstones (Palain, 1979). The **São Bartolomeu de Messines Clays** are present at the base of the unit and are composed of pelites. The sedimentary facies and

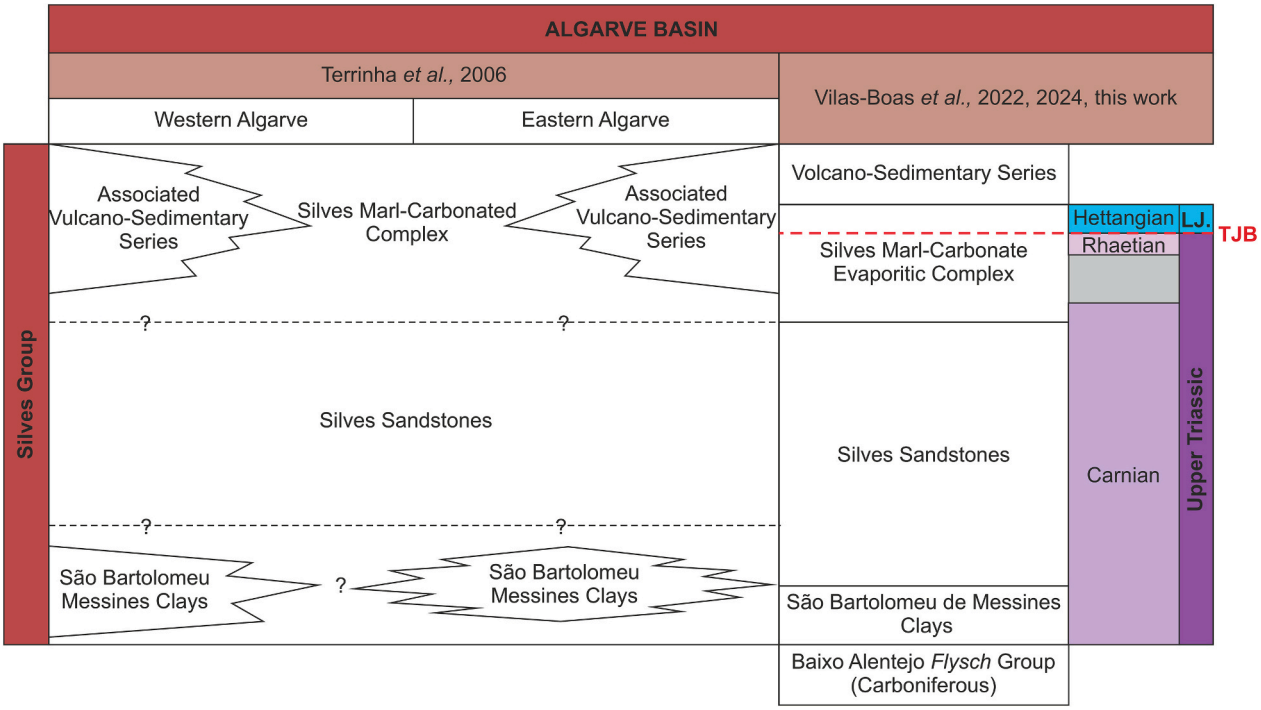

Fig. 3. Lithostratigraphical scheme of the Silves Group in the Algarve Basin with the new age data (adapted from Terrinha et al., 2006). LJ. – Lower Jurassic. TJB – Triassic–Jurassic Boundary.

structures of this unit indicate a fluvial depositional environment. Moreover, the absence of thick pelitic intercalations, typically attributed to floodplain deposits, and the lack of thick pelitic intercalations generally associated with floodplain deposits, suggest deposition within braided river systems.

The **Silves Marl–Carbonate Evaporitic Complex,** the upper portion of the Group, consists of variegated mudstones interbedded with marls, fine-grained sandstones, siltstones, and pelites. South of the Sagres-Algoz-Tavira alignment, this unit includes a thick evaporitic succession, currently explored in the Loulé Diapir (Terrinha et al., 2013). The fossil assemblages and sedimentary features suggest deposition in a shallow lacustrine environment subjected to periodic desiccation (ephemeral lakes).

The **Volcano–Sedimentary Series** consists of alternating layers of tuffites, cinerites, pyroclastic material, and occasional basalt flows, reflecting a dominance of explosive over effusive volcanic activity. This magmatic event aligns with the first extensional tectonic pulse associated with the opening of the Central Atlantic Ocean (Terrinha et al., 2013).

2.2. *Lusitanian Basin*

The Lusitanian Basin developed along the Western Iberian Margin during the Mesozoic (Figs. 1 and 2). Its origin and evolution are closely linked to the tectonic reactivation of Variscan basement structures during successive rifting phases of Pangaea, ultimately leading to the opening of the North Atlantic Ocean, from the Middle?–Late Triassic to the latest Early Cretaceous (Wilson, 1975, 1988; Hiscott et al., 1990; Kullberg et al., 2013). During the Middle?–Late Triassic, the basin was infilled predominantly by siliciclastic deposits of the Silves Group, including coarse-grained pebbly arkoses and feldspathic litharenites (Palain, 1976; Soares et al., 2007, 2012).

The Silves Group has been the focus of several studies in the Lusitanian Basin (e.g., Carvalho, 1950; Palain, 1976, 1979). The type-section of this unit was first described in the Coimbra region by Choffat (1903) and informally referred to as the "Grés de Silves," later redefined by Palain (1976) and Soares et al. (2012).

In the most recent lithostratigraphical framework, compiled for the Geological Map of Portugal (Coimbra-Lousã, sheet 19-D, 1:50,000 scale), the Silves Group in the Lusitanian Basin is subdivided, in ascending stratigraphical order, into the Conraria, Penela, Castelo Viegas, and Pereiros formations (Soares et al., 2007, 2012; Fig. 4). A more detailed description of the units of the Silves Group in the Lusitanian Basin is presented in Supplementary Material A.

The **Conraria Formation** unconformably overlies either upper Precambrian or, locally, Carboniferous rocks and comprises ferruginous conglomerates and sandstones (Palain, 1976; Soares et al., 2012). This unit has been interpreted as deposited in a transgressive alluvial plain-lacustrine setting that developed under arid climatic conditions, with localized saline and carbonate flooding and short-lived episodes of intense precipitation (Palain, 1976; Soares et al., 2012).

The **Penela Formation** (=base of term B1 of Palain, 1976) consists of reddish to brownish sandy conglomerates deposited in a river system evolving from braided to meandering (Palain, 1976; Soares et al., 2012).

The **Castelo Viegas Formation** comprises beds of microconglomerates and coarse-grained arkoses interbedded with rare centimetre-thick, muddy layers, deposited in a transgressive evolution from braided to meandric system (Palain, 1976; Soares et al., 2012).

The uppermost unit, the **Pereiros Formation**, at its base comprises fine crystalline dolostones interbedded with siliciclastics, and millimetre to centimetre-thick mudstones. The upper part of the formation consists of reddish to greyish sandy mudstones, fine-grained dolostones and dolomitic marls with patchy gypsum lenses, and culminates at the top with laminated dolostones (Azerêdo et al., 2003; Sêco et al., 2015). This formation was deposited in a shallow evaporitic lagoonal environment that evolved into a coastal lagoon setting bounded by sandy barrier islands (Soares et al., 2012).

Overlying the Silves Group, more specifically the Pereiros Formation, and marked by another significant facies change is the Coimbra Formation, composed by dolostones, dolomitic limestones and limestones (Azerêdo et al., 2003, 2014; Dimuccio et al., 2014, 2016; Duarte et al., 2014, 2022; Gómez et al., 2019).

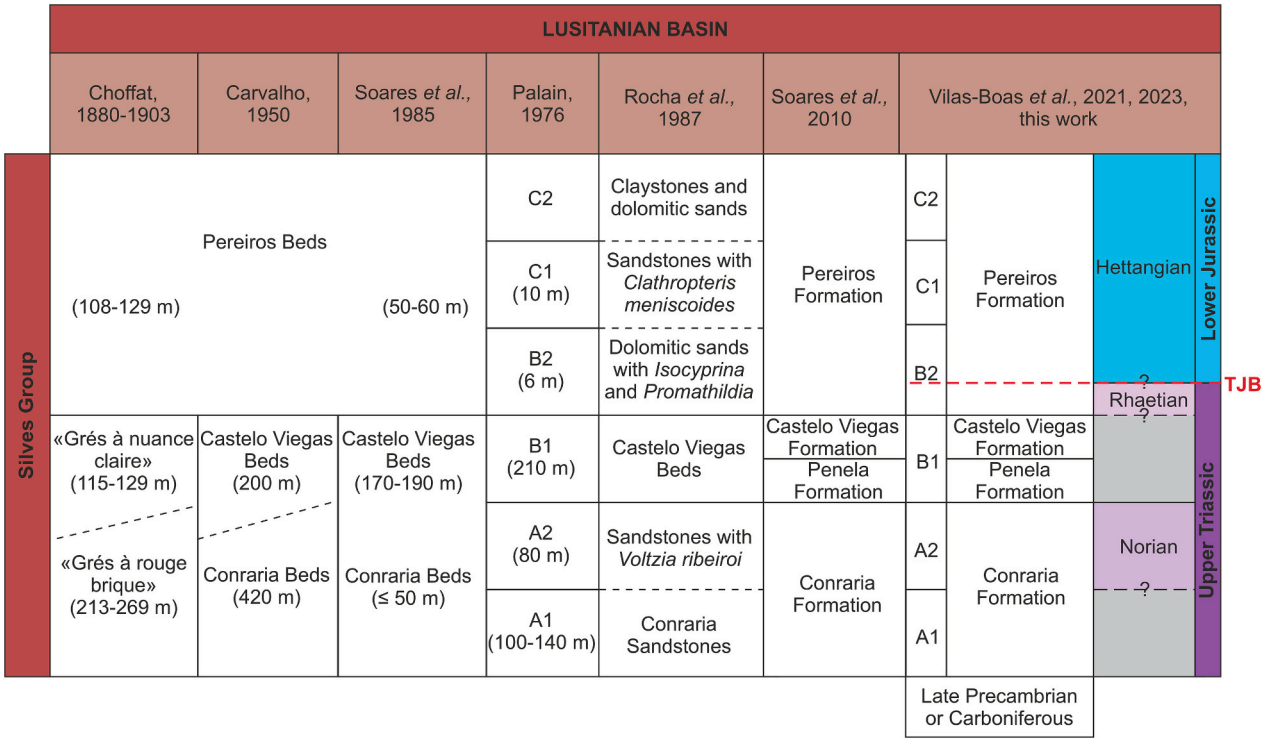

Fig. 4. Lithostratigraphical organisation of the Silves Group in the Lusitanian Basin with the new age data (adapted from Kullberg et al., 2013). TJB – Triassic–Jurassic Boundary.

The earliest palynostratigraphical study was carried out by Doubinger et al. (1970) and later expanded upon by Adloff et al. (1974). These works were grounded in the sedimentological and allostratigraphical framework established by Palain (1976, 1979). Subsequently, Díez (2000) conducted new palynological analyses, based mainly on the same outcrops, assigning an early to middle Carnian age to the Conraria Formation, a middle Carnian to late Norian age to the Penela and Castelo Viegas formations, and a Hettangian to Sinemurian age to the Pereiros Formation. More recently, however, Díez (2000) and Arche and López-Gómez (2014) revised the age of the Pereiros Formation to late Norian-early Rhaetian. Improved age constraints have been provided by recent palynological data from these strata, which date the Conraria Formation to the Norian (Late Triassic) and the Pereiros Formation to the Hettangian (Early Jurassic) (Vilas-Boas et al., 2021).

3. Materials and methods

3.1. Studied sections

The sections selected for this study represent the most lithostratigraphically complete successions of the Upper Triassic and Lower Jurassic in each basin. Sampling focused on lithologies more suitable for palynological analysis, particularly mudrocks. Previously biostratigraphical frameworks guided the selection of key intervals and sections. Field sampling was conducted across the Algarve and Lusitanian basins. Six boreholes were also sampled Campelos-1, Golfinho-1, Lula-1, Santiago do Cacém-3, Santiago do Cacém-42, and Santiago do Cacém-61 at the Laboratório Nacional de Energia e Geologia (LNEG - Geological Survey to obtain better-preserved palynological material from Upper Triassic and Lower Jurassic.

The sections are described below, organized by basin and subdivided by lithostratigraphical unit or formation.

3.1.1. Algarve Basin

A total of two hundred and fifty-four samples (254 samples) encompassing both the Upper Triassic and Lower Jurassic strata were collected from fifteen composite sections across the Algarve Basin for palynological investigation. Due to lithostratigraphy, most of the samples collected in this basin belong to the Upper Triassic, with only a limited number derived from the lowermost Jurassic. From the Silves Sandstones, a total of eighty-seven samples were collected from eight sections, and from the Silves Marl–Carbonate Evaporitic Complex, a total of one hundred sixty-seven samples were collected from eight sections. Palynologically productive samples from the Silves Sandstones were obtained from Amado's Beach, Amorosa and the International Racetrack of Algarve sections (Table 1). In the Silves Marl–Carbonate Evaporitic Complex, productive samples were recovered from the Albufeira Diapir, Amado's Beach, and Loulé Rock Salt Mine sections (Table 1).

3.1.2. Lusitanian Basin

The lithology in the Lusitanian Basin was more favourable for palynological investigations, allowing for the collection of diverse sediments spanning the Upper Triassic and Lower Jurassic. A total of one hundred and twenty-two samples (122 samples) were collected from twelve composite sections distributed across the basin and analysed for their palynological content. The Penela Formation was not sampled because its lithofacies were unsuitable for palynological analysis. Three sections within the middle to upper part of the Conraria Formation were sampled, yielding a total of eleven samples. The Castelo Viegas Formation was sampled across four sections, yielding a total of 14 samples. Given its favourable lithology, the Pereiros Formation yielded the highest number of samples in the Lusitanian Basin, with a total of ninety-five samples collected across multiple sections. Two samples were collected from the Coimbra Formation in the Carvalhais section (Coimbra), which also proved for helping to constrain the Pereiros Formation stratigraphically.

Palynologically productive samples were recovered from the Conraria, Pereiros and base of the Coimbra formations. In the Conraria Formation, productive samples were recovered in the Alto de São João,

Table 1
Geographical coordinates and summary of the number of studied samples in each section of the Algarve and Lusitanian Basin and their productivity in percentage. The totals are also presented.

Algarve Basin				
Section	Geographic coordinates	N° Collected Samples	N° Productive Samples	Productivity %
Albufeira's Diapir	N37°4′54.18″; W8°15′45.27”	4	2	50
Amado's Beach	N37°10′9.37″; W8°54′10.72”	20	2	10
Amorosa	N37°15′38.65″; W8°16′11.66”	17	1	5.9
	N37°15′35.05″; W8°19′32.00”			
	N37°15′35.71″; W8°19′32.13”			
Ayamonte	N37°13′36.94″; W7°24′28.16”	9	0	0
Barragem do Funcho	N37°15′6.58″; W8°21′6.70”	4	0	0
Bengado	N37°9′31.70″; W7°50′39.84”	9	0	0
Bodega	N37°9′24.96″; W7°40′33.38”	3	0	0
Fonte da Pedra	N37°10′46.99″; W8°38′3.30”	1	0	0
International Racetrack of Algarve	N37°11′12.31″; W8°38′10.82”	24	10	41.7
Loulé Rock Salt Mine	N37°8′5.53″; W8°0′28.05”	33	9	27.3
Marco	N37°8′59.27″; W7°44′59.66”	6	0	0
Rocha da Pena	N37°15′1.15″; W8°6′28.42”	15	0	0
	N37°15′0.43″; W8°6′30.73”			
	N37°14′58.56″; W8°6′33.93”			
	N37°15′1.05″; W8°6′38.93”			
Santa Catarina Fonte do Bispo	N37°9′14.24″; W7°47′45.03”	6	0	0
Santa Rita	N37°10′45.36″; W7°33′44.78”	15	0	0
Vale Fuzeiros	N37°15′13.30″; W8°20′25.61”	88	0	0
	TOTAL	254	24	8.99
Lusitanian Basin				
Section	Geographic coordinates	N° Collected Samples	N° Productive Samples	Productivity %
Alto de São João	N40°11′23.57″; W8°24′6.14”	3	2	66.7
Carvalhais	N40°10′21.59″; W8°26′8.67”	2	2	100
Castelo Viegas I	N40°9′48.58″; W8°24′26.61”	3	1	33.3
Castelo Viegas II	N40°9′47.63″; W8°24′28.99”	3	0	0
Eiras	N40°14′50.13″; W8°24′35.45”	2	0	0
Ideal Med	N40°13′30.55″; W8°25′24.97”	2	0	0
Lamas I	N40°4′44.35″; W8°22′48.30”	25	15	60
Lamas II	N40°5′6.42″; W8°23′10.30”	12	10	83.3
Lordemão	N40°13′57.48″; W8°24′52.44”	51	6	11.8
Parque de Campismo	N40°11′25.78″; W8°23′59.21”	3	2	66.7
Redonda	N40°14′41.34″; W8°24′38.29”	11	0	0
Sobral Cid	N40°10′27.20″; W8°23′59.91”	5	3	60
	TOTAL	122	41	40.15

Parque de Campismo and Sobral Cid sections (Table 1). For the Pereiros Formation, productive samples were obtained from the Castelo Viegas II, Lamas I, Lamas II and Lordemão sections (Table 1). The Carvalhais section, the only one sampled for the Coimbra Formation, was palynologically productive (Table 1).

3.2. Palynology

Standard palynological procedures were followed for sample preparation, including acid digestion with hydrochloric acid (HCl) and hydrofluoric acid (HF), followed by the subsequent concentration of organic matter. The methodologies described by Wood et al. (1996) and Riding and Warny (2008) were applied. Of the 376 samples processed, 65 yielded palynomorphs, ranging from moderately to well-preserved, accounting for approximately 17% of the productive samples. The organic residues were sieved through a 15 μm mesh and mounted on microscope slides using Entelan®, a commercial resin-based mounting medium. Semi-quantitative abundance data were obtained by counting two hundred and fifty specimens per slide. Two to three slides per sample were examined for the presence of rare taxa, which were identified but excluded from the quantitative counts. Samples processing was carried out at the Geological Survey of Portugal (LNEG) and at the Centre for Marine and Environmental Research, the University of Algarve (CIMA-UAlg). Microscopic analysis was conducted under transmitted light using an Olympus BX40 microscope equipped with an Olympus C5050 digital camera, as well as a Leica DM750 microscope paired with a Leica ICC50W camera. All samples, residues, and mounted slides are currently stored in the collection of LNEG, at S. Mamede de Infesta and CIMA-UAlg, at Faro (Portugal). The taxonomy adopted in this study follows the classical morphological framework commonly used in Triassic–Jurassic biostratigraphy (e.g., Scheuring, 1970; Morbey, 1975; Cirilli, 2010). We acknowledge the recent taxonomic revision of the *Enzonalasporites* group by Scibiorski et al. (2022), which emended diagnoses and synonymized several species based on ultrastructural and high-resolution morphological criteria. However, given that our determinations are based on transmitted light microscopy and routine palynological criteria, and in order to maintain consistency with the regional biostratigraphical framework, we retain the traditional taxonomic assignments while noting their revised status where relevant.

4. Palynostratigraphy of the Silves Group

The data obtained in this study represent a significant contribution to the stratigraphical palynology of the Triassic-Jurassic transition in Portugal. A total of thirty-one genera and twenty-five species of pollen, twenty-nine genera and seventeen species of spores and six genera and two species of algae were identified across twenty-seven sections in the Algarve and Lusitanian basins. These palynological assemblages are described and illustrated in Figs. 5 to 9.

The quantitative and qualitative distribution of these assemblages is presented based on the relative abundance of key taxa, along with the first and last occurrences (FO; LO) and first and last appearance datum (FAD; LAD) of specific stratigraphically significant taxa (Figs. 10, 11 and 12). A list of all the taxa found in the studied samples is provided in

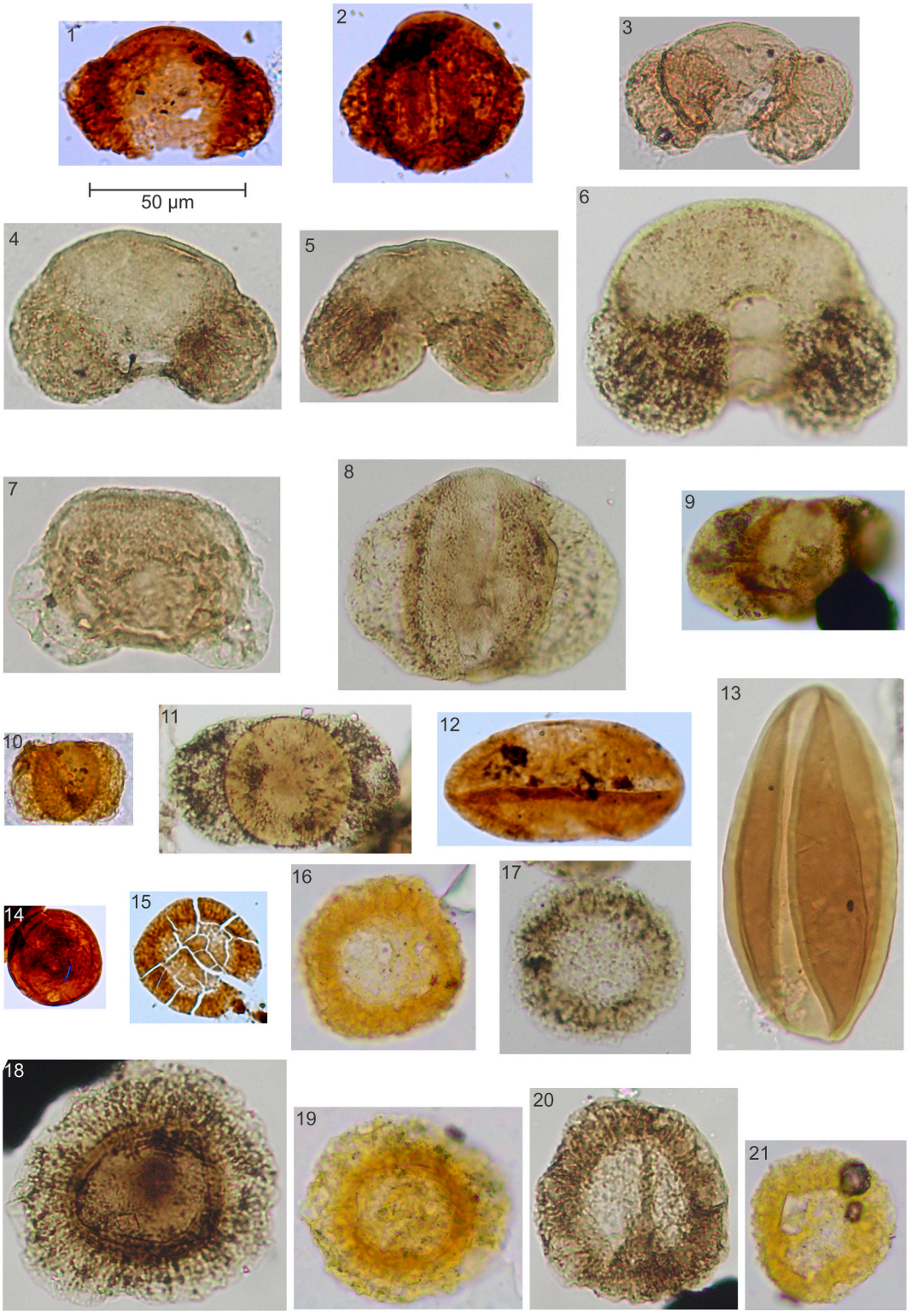

(caption on next page)

Fig. 5. Selected pollen grains from the Silves Group sections in the Algarve and Lusitanian basins, studied in this work. Species name is followed by the sample, section, palynozone, unit/formation and basin.
1.?*Klausipollenites* sp., sample AUTO3, International Racetrack of Algarve section, AT palynozone, Silves Sandstones, Algarve Basin.
2.?*Protodiploxypinus* sp., sample AUTO3, International Racetrack of Algarve section, AT palynozone, Silves Sandstones, Algarve Basin.
3. *Samaropollenites speciosus* Goubin 1965, sample AM15, Amado's Beach section, SC palynozone, Silves Marl–Carbonate Evaporitic Complex, Algarve Basin.
4. *Samaropollenites speciosus* Goubin 1965, sample PC2, Parque de Campismo section, CG palynozone, Conraria Formation, Lusitanian Basin.
5. *Microcachrydites doubingeri* Klaus 1964, sample PC1, Parque de Campismo section, CG palynozone, Conraria Formation, Lusitanian Basin.
6. *Microcachrydites fastidioides* (Jansonius) Klaus 1964, sample PC2, Parque de Campismo section, CG palynozone, Conraria Formation, Lusitanian Basin.
7. *Pinuspollenites minimus* (Couper) Kemp 1970, sample LAM8, Lamas II section, Pm palynozone, Pereiros Formation, Lusitanian Basin.
8. *Alisporites* sp., sample PC2, Parque de Campismo section, CG palynozone, Conraria Formation, Lusitanian Basin.
9. *Alisporites diaphanus* (Pautsch 1958) Lund 1977, sample MSGvd7, Loulé Rock Salt Mine section, CP palynozone, Silves Marl–Carbonate Evaporitic Complex, Algarve Basin.
10. *Triadispora* sp., sample Amorosa4(−20 cm), Amorosa section, SC palynozone, Silves Sandstones, Algarve Basin.
11. *Triadispora staplini* (Jansonius) Klaus 1964, sample PC2, Parque de Campismo section, CG palynozone, Conraria Formation, Lusitanian Basin.
12. *Ovalipollis pseudoalatus* Krutzsch 1955, sample AUTO3, International Racetrack of Algarve section, AT palynozone, Silves Sandstones, Algarve Basin.
13. *Cycadopites* sp., sample LAM2, Lamas II section, Pm palynozone, Pereiros Formation, Lusitanian Basin.
14. *Aulisporites astigmosus* (Leschik 1956) Klaus 1960, sample AUTO3, International Racetrack of Algarve section, AT palynozone, Silves Sandstones, Algarve Basin.
15. *Tuleposrites briscoensis* Dunay & Fischer 1979, sample AUTO3, International Racetrack of Algarve section, AT palynozone, Silves Sandstones, Algarve Basin.
16. *Enzonalasporites vigens* Leschik 1956 emend. Scheuring, 1970, sample AM15, Amado's Beach section, SC palynozone, Silves Marl–Carbonate Evaporitic Complex, Algarve Basin.
17. *Enzonalasporites vigens* Leschik 1956 emend. Scheuring, 1970, sample PC2, Parque de Campismo section, CG palynozone, Conraria Formation, Lusitanian Basin.
18. *Patinasporites densus* Leschik emend. Scheuring, 1970, sample AM16, Amado's Beach section, SC palynozone, Silves Marl–Carbonate Evaporitic Complex, Algarve Basin.
19. *Patinasporites densus* Leschik emend. Scheuring, 1970, sample PC1, Parque de Campismo section, CG palynozone, Conraria Formation, Lusitanian Basin.
20. *Vallasporites ignacii* Leschik 1956 emend. Scheuring, 1970, sample AM16, Amado's Beach section, SC palynozone, Silves Marl–Carbonate Evaporitic Complex, Algarve Basin.
21. *Vallasporites ignacii* Leschik 1956 emend. Scheuring, 1970, sample PC1, Parque de Campismo section, CG palynozone, Conraria Formation, Lusitanian Basin.

Supplementary Material B.

Overall, the Lower Jurassic samples proved to be more productive than those from the Upper Triassic. In addition to outcrop samples, 122 samples from six boreholes were analysed to retrieve potential better-preserved material from the Upper Triassic and Lower Jurassic; however, all borehole samples were barren. Consequently, this research focuses on the two Portuguese basins that yielded the most representative Upper Triassic to Lower Jurassic palynological material. In both basins, these records mark the beginning of the Mesozoic megacycle associated with the breakup of the Pangaea, commonly characterised by basal siliciclastic units and continental red beds. The depositional environments begin as fluvial at the base, then transition to coastal areas, such as pond lagoons and sabkha (Algarve Basin), and to estuarine and evaporitic tidal settings (Lusitanian Basin).

The following sections present the palynoassemblages arranged in stratigraphical order, from the oldest to youngest, integrating their taxonomic composition with the definition of new palynozones to highlight temporal changes in floral diversity and facilitate regional correlation.

4.1. Algarve Basin

For the first time, three palynozones, from the oldest to the youngest, are proposed for the Silves Group of the Algarve Basin, based on the abundance, FO and LO of key palynomorph taxa (Figs. 10 and 11), and integrated with the palynozonations previously established and discussed by Vilas-Boas et al. (2021, 2023).

4.1.1. *Aulisporites astigmosus – Tulesporites briscoensis (AT) palynozone*

Data and composition: The microflora was recovered from the International Racetrack of Algarve section assigned to the Silves Sandstones. It comprises moderately to well-preserved sporomorphs, including eleven genera and six species of pollen, and seven genera and two species of spores. This assemblage is characterized by the common to abundant occurrence of the pollen taxa *Aulisporites astigmosus* and *Tulesporites briscoensis* (Dunay and Fisher, 1979) = *Enzonalasporites ignacii* sensu Scibiorski et al. (2022), together with the spores *Calamospora* sp., *Conbaculatisporites* sp., *Converrucosisporites* sp., *Deltoidospora* sp., *Lycopodiacidites rugulatus, Nevesisporites* cf. *vallatus,* and *Verrucosisporites* sp.. Rare accompanying taxa include the species *Cycadopites* sp., *Enzonalasporites vigens, Alisporites* sp., *Klausipollenites* sp., *Ovalipollis pseudoalatus, Protodiploxypinus* sp., *Samaropollenites speciosus, Triadispora* sp. and *Vallasporites ignacii* (Leschik, 1956 emend. Scheuring, 1970) = *Enzonalasporites ignacii* sensu Scibiorski et al. (2022).

Age: This palynozone is marked by the presence of *Alisporites* sp., *Aulisporites astigmosus, Cycadopites* sp., *Enzonalasporites vigens, Nevesisporites* cf. *vallatus, Ovalipollis pseudoalatus*,?*Protodiploxypinus* sp., *Samaropollenites speciosus, Triadispora* sp., *Tulesporites briscoensis*, and *Vallasporites ignacii*. Associated spores include *Calamospora* sp., *Conbaculatisporites* sp., *Converrucosisporites* sp., *Deltoidospora* sp.,?*Klausipollenites* sp., *Lycopodiacidites rugulatus* and *Verrucosisporites* sp. The fact that *Aulisporites astigmosus* is present together with *Enzonalasporites vigens, Samaropollenites speciosus* and *Tulesporites briscoensis* indicates an early Carnian age. The recovered palynoflora assemblage presents a mixed signature, featuring typical microflora elements characteristic of Central Europe and North America. This data is consistent with the palaeogeographical position of the Iberian Peninsula during this period (Palain, 1976; Terrinha et al., 2013; Vilas-Boas et al., 2022).

4.1.2. *Samaropollenites speciosus – Camerosporites secatus (SC) palynozone*

Data and composition: This assemblage was recovered from the Silves Sandstones and Silves Marl–Carbonate Evaporitic Complex, cropping out at the Amorosa and Amado Beach sections, respectively. It comprises twelve genera and ten species of pollen, five genera and one species of spores, and four genera and two species of algae, all moderately to well-preserved. The assemblage is characterized by the simultaneous occurrence of *Enzonalasporites vigens, Samaropollenites speciosus, Vallasporites ignacii, Patinasporites densus* and *Granuloperculatipollis rudis,* the latter two making their FO in this palynoassemblage. Other consistently present taxa include *Paracirculina* sp., *Paracirculina quadruplicis, Playfordiaspora* sp. and *Triadispora* sp.. Additional components include the pollen *Alisporites* sp., *Camerosporites secatus, Ellipsovelatisporites* sp., *Lagenella martinii, Microcachrydites doubingeri, Microcachrydites fastidioides, Microcachrydites* sp., as well as malformed specimens of *Paracirculina* sp., and the spores *Calamospora* sp., *Convolutispora* sp., *Kraeuselisporites reissingeri* and *Verrucosisporites* sp.. The algal component comprises *Botryococcus* sp., *Leiosphaeridia* sp., *Ovoidites* sp.,

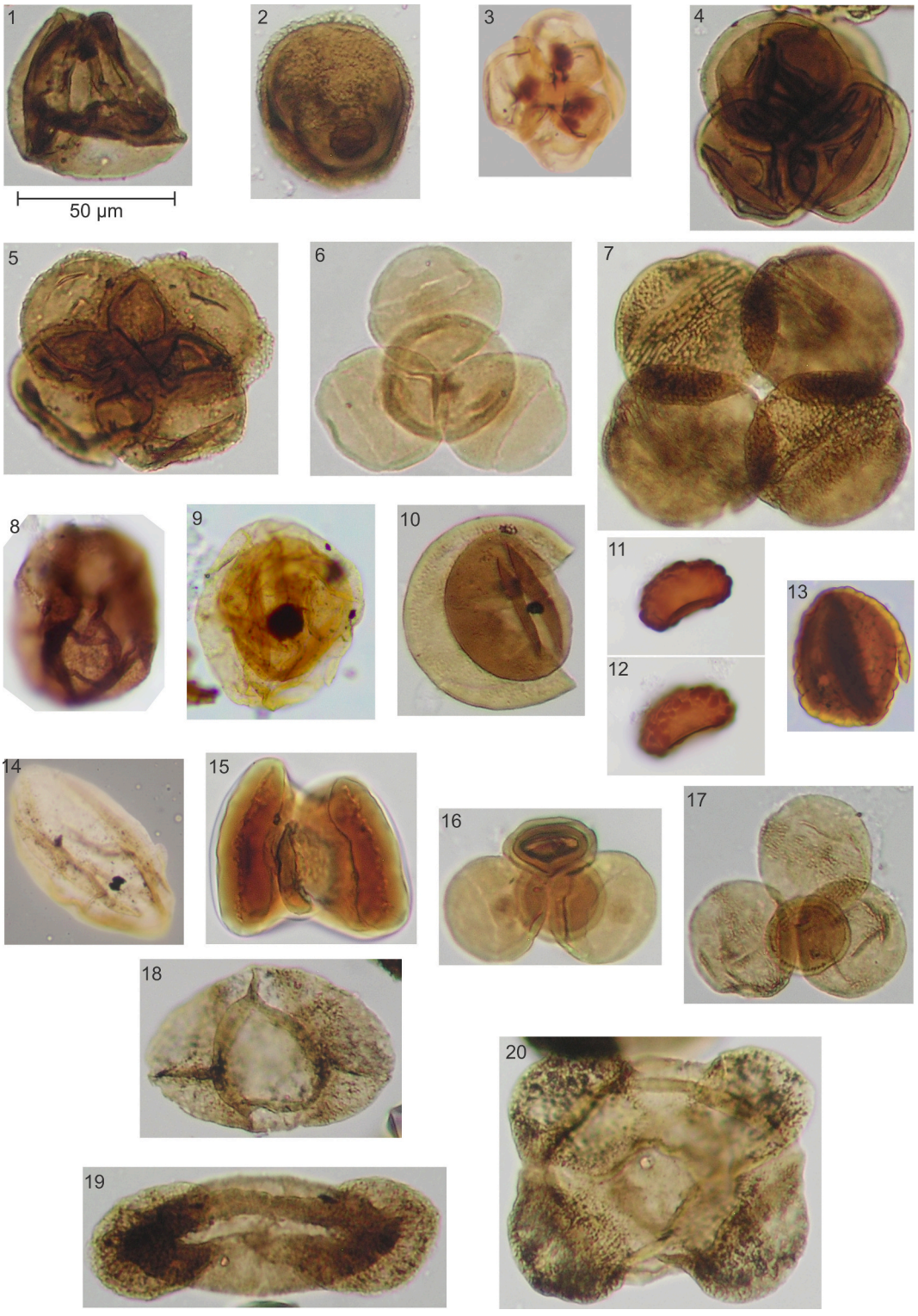

(caption on next page)

Fig. 6. Selected pollen grains (1–15) and malformed sporomorphs (16–20) from the Silves Group sections in the Algarve and Lusitanian basins, studied in this work. Species name is followed by the sample, section, palynozone, unit/formation and basin.
1. *Duplicisporites granulatus* Leschik 1955 emend. Scheuring, 1970, sample PC2, Parque de Campismo section, CG palynozone, Conraria Formation, Lusitanian Basin.
2. *Granuloperculatipollis rudis* Venkatachala & Góczán emend. Morbey, 1975, sample ASJ2, Alto de São João section, CG palynozone, Conraria Formation, Lusitanian Basin.
3. *Paracirculina quadruplicis* Scheuring, 1970, sample AM15, Amado's Beach section, SC palynozone, Silves Marl–Carbonate Evaporitic Complex, Algarve Basin.
4. *Paracirculina quadruplicis* Scheuring, 1970, sample PC1, Parque de Campismo section, CG palynozone, Conraria Formation, Lusitanian Basin.
5. *Praecirculina granifer* (Leschik) Klaus 1960, sample PC1, Parque de Campismo section, CG palynozone, Conraria Formation, Lusitanian Basin.
6. *Classopollis meyerianus* (Klaus) de Jersey 1973, sample LAM6, Lamas II section, Pm palynozone, Pereiros Formation, Lusitanian Basin.
7. *Classopollis torosus* Reissinger 1950, sample LAM12, Lamas II section, Pm palynozone, Pereiros Formation, Lusitanian Basin.
8. *Araucariacites australis* Cookson 1947, sample MSGvdBASE, Loulé Rock Salt Mine section, CP palynozone, Silves Marl–Carbonate Evaporitic Complex, Algarve Basin.
9. *Perinopollenites elatoides* Couper 1958, sample MSGvd7, Loulé Rock Salt Mine section, CP palynozone, Silves Marl–Carbonate Evaporitic Complex, Algarve Basin.
10. *Perinopollenites elatoides* Couper 1958, sample LAM12, Lamas II section, Pm palynozone, Pereiros Formation, Lusitanian Basin.
11. *Cerebropollenites* sp., sample MSGvd6, Loulé Rock Salt Mine section, CP palynozone, Silves Marl–Carbonate Evaporitic Complex, Algarve Basin.
12. *Cerebropollenites* sp., sample MSGvd6, Loulé Rock Salt Mine section, CP palynozone, Silves Marl–Carbonate Evaporitic Complex, Algarve Basin.
13. *Cerebropollenites macroverrucosus* (Thiergart) Schulz 1967, sample MSGvd6, Loulé Rock Salt Mine section, CP palynozone, Silves Marl–Carbonate Evaporitic Complex, Algarve Basin.
14. *Ephedripites* sp., sample MSGvd8, Loulé Rock Salt Mine section, CP palynozone, Silves Marl–Carbonate Evaporitic Complex, Algarve Basin.
15. *Rhaetipollis germanicus* Schulz 1967, sample LAG27b, Lordemão section, IK palynozone, Pereiros Formation, Lusitanian Basin.
16. *Classopollis meyerianus* (Klaus) de Jersey 1973, sample LAM2, Lamas II section, Pm palynozone, Pereiros Formation, Lusitanian Basin. Tetrad with two malformed *Classopollis* pollen grains.
17. *Classopollis torosus* Reissinger 1950, sample LAM2, Lamas II section, Pm palynozone, Pereiros Formation, Lusitanian Basin. Tetrad with one malformed *Classopollis* pollen grain.
18. Malformed pollen grain, sample PC2, Parque de Campismo section, CG palynozone, Conraria Formation, Lusitanian Basin.
19. Malformed pollen grain, sample PC2, Parque de Campismo section, CG palynozone, Conraria Formation, Lusitanian Basin.
20. Malformed pollen grain, sample PC2, Parque de Campismo section, CG palynozone, Conraria Formation, Lusitanian Basin.

Plaesiodictyon mosellanum ssp. *bullatum, Plaesiodictyon mosellanum* ssp. *variable, Plaesiodictyon* sp., and an undetermined species named Algae sp. A.

Age discussion: The SC palynozone is distinguished by a high abundance of Circumpolles, *Paracirculina quadruplicis, Paracirculina* sp., *Camerosporites secatus, Enzonalasporites vigens, alongside* the monosaccate pollen *Patinasporites densus* and the bisaccate *Samaropollenites speciosus,* supporting a Carnian age as observed in the European domain (Schuurman, 1977, 1979; Dolby and Balme, 1976; Buratti and Cirilli, 2007; Mehdi et al., 2009; Cirilli, 2010; Kürschner and Herngreen, 2010; Buratti et al., 2012; Mietto et al., 2012). The LAD of *Camerosporites secatus* that in the Central and North-Western Europe, marks the Carnian-Norian boundary (Cirilli, 2010; Kürschner and Herngreen, 2010) and the additional presence of *Ellipsovelatisporites* sp., *Triadispora* sp. and *Vallasporites ignacii,* further constrains the assemblage to the upper Carnian (Schuurman, 1977, 1979; Visscher and Krystyn, 1978; Visscher et al., 1980; Visscher and Brugman, 1981; Van der Eem, 1983; Fisher and Dunay, 1984; Blendinger, 1988; Hochuli et al., 1989; Cirilli and Eshet, 1991; Cirilli and Montanari, 1994; Broglio Loriga et al., 1999; Hochuli and Frank, 2000; Warrington, 2002; Roghi, 2004; Mietto et al., 2007; Cirilli, 2010). Additionally, the presence of *Granuloperculatipollis rudis,* whose FO lies in the Tuvalian (Kürschner and Herngreen, 2010; Mietto et al., 2012; Kustatscher et al., 2018), and *Lagenella martinii,* whose LO in Europe is referred to the same age (Kürschner and Herngreen, 2010), reinforces the assignment of this palynozone to the upper Carnian.

4.1.3. *Cerebropollenites macroverrucosus – Perinopollenites elatoides (CP) palynozone*

Data and composition: This palynozone is based in the combination of two assemblages, both obtain in the Loulé Rock Salt Mine section, belonging to the Silves Marl–Carbonate Evaporitic Complex. The first material was recovered in the lower part of the Loulé Rock Salt Mine and is moderately to well-preserved. Includes six genera and three species of pollen, two genera and one species of spores, and one genus and one species of algae. A defining feature of this assemblage is the FO of the *Classopollis meyerianus* and *Classopollis* sp.. Additional pollen are *Alisporites* sp., *Araucariacites australis, Araucariacites* sp., *Cycadopites* sp., *Paracirculina quadruplicis, Triadispora* sp., and the spores *Calamospora mesozoica* and *Playfordiaspora* sp.. Notably, specimens with fungal or algal affinity were also recorded in all productive samples. The darker colour of these forms, which resemble Neoproterozoic algae (e.g., *Ourasphaira giraldae*), suggests that they may be part of reworked material derived from older rocks. The remaining material was collected from the upper part of the Loulé Rock Salt Mine section and comprises a total of seven genera and six species of pollen, six genera and four species of spores, and one genus of algae, all of which show moderate to good preservation. The assemblage is distinguished by the FO of *Cerebropollenites macroverrucosus* (Thiergart) Schulz, 1967 sensu lato (= *Sciadopityspollenites macroverrucosus* comb. nov. et emend. Gravendyck et al., 2023), *Cerebropollenites* sp., and *Perinopollenites elatoides* and the spores *Kraeuselisporites reissingeri* and *Leptolepidites argenteaeformis*. Additional pollen includes *Alisporites diaphanus, Araucariacites australis, Araucariacites* sp., malformed specimens of *Classopollis* sp., *Classopollis meyerianus, Classopollis torosus, Classopollis* sp., *Cycadopites* sp., and *Ephedripites* sp.. Other spores are *Anapiculatisporites* sp., *Calamospora mesozoica, Calamospora* sp., *Deltoidospora* sp., *Deltoidospora toralis, Kraeuselisporites* sp. and *Kyrtomisporis* sp.. The algae *Leiosphaeridia* sp. was also identified.

Age discussion: This palynozone is mainly characterised by *Araucariacites* sp., *Classopollis meyerianus,* and *Classopollis torosus,* with a significant increase in *Kraeuselisporites reissingeri.* At the basal part, it is noteworthy that Hettangian taxa are absent, along with the typical Carnian to upper Norian elements (such as *Camerosporites* spp., *Ellipsovelatisporites* spp., *Enzonalasporites* spp., *Patinasporites densus, Rhaetipollis germanicus, Vallasporites ignacii,* and *Granuloperculatipollis rudis*), indicating that this section dates to the upper Rhaetian (Morbey, 1975; Schuurman, 1977, 1979; Visscher et al., 1980; Fisher and Dunay, 1981; Visscher and Brugman, 1981; Cirilli, 2010). However, at the top of the sampled section, the first occurrence (FO) of *Cerebropollenites macroverrucosus, Cerebropollenites* sp., and *Perinopollenites elatoides,* suggests a Hettangian age. Therefore, it is possible to identify the TJB within this palynozone, as observed in other sections across Europe (Clement-Westerhof et al., 1974; Morbey, 1975, 1978; Van Erve, 1977; Visscher et al., 1980; Fisher and Dunay, 1981; Kürschner et al., 2007; Kürschner and Herngreen, 2010). Based on the palynological data, this palynozone can be assigned to the upper Rhaetian to the lowermost Hettangian.

The palynoassemblage recovered from the Albufeira Diapir is

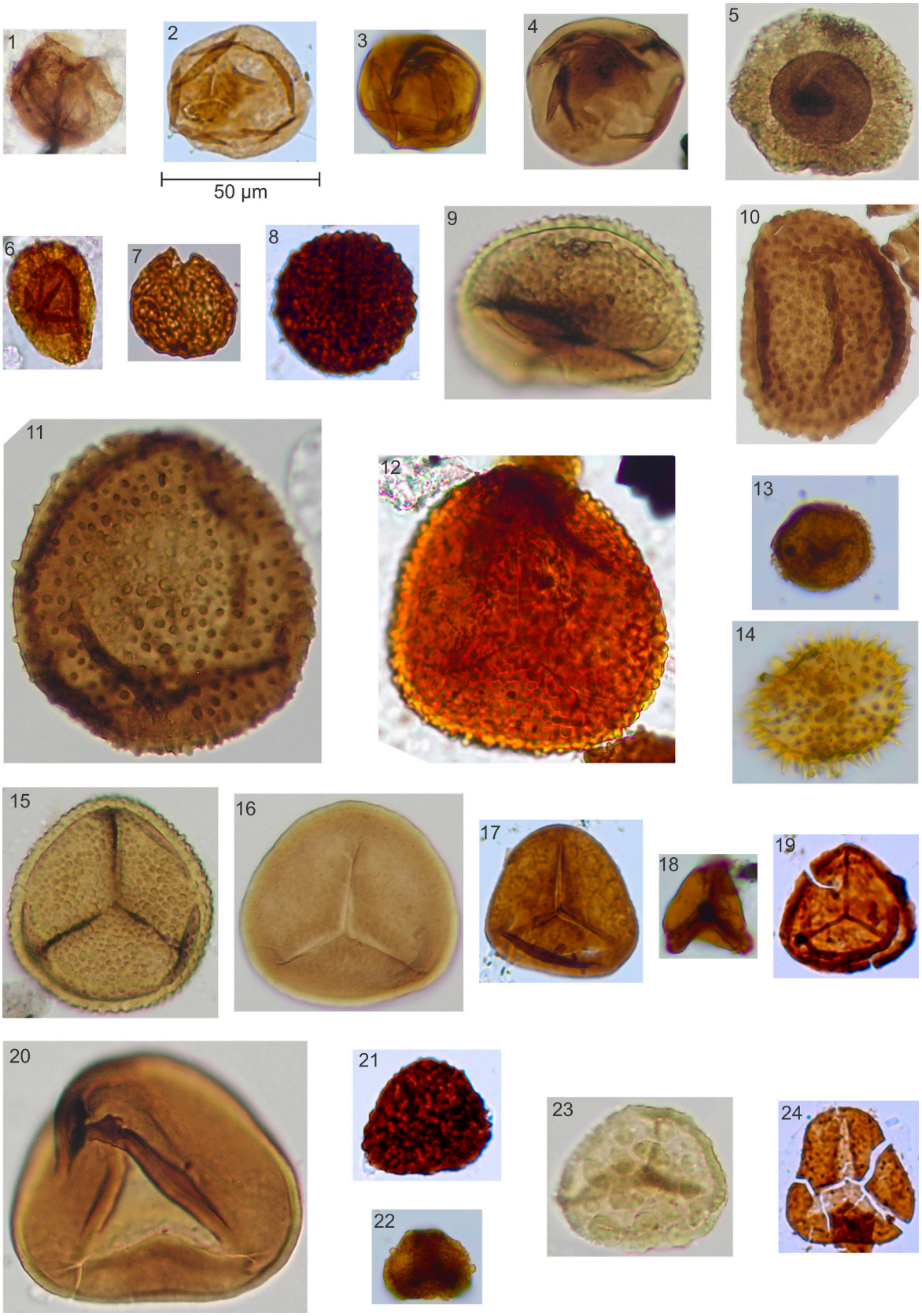

(caption on next page)

Fig. 7. Selected spores from the Silves Group sections in the Algarve and Lusitanian basins, studied in this work. Species name is followed by the sample, section, palynozone, unit/formation and basin.
1. *Calamospora mesozoica* Couper 1958, sample MSGvd1, Loulé Rock Salt Mine section, CP palynozone, Silves Marl–Carbonate Evaporitic Complex, Algarve Basin.
2. *Calamospora* sp., sample AUTO3, International Racetrack of Algarve section, AT palynozone, Silves Sandstones, Algarve Basin.
3. *Calamospora tener* (Leschik) Mädler 1964, sample MSGvd7, Loulé Rock Salt Mine section, CP palynozone, Silves Marl–Carbonate Evaporitic Complex, Algarve Basin.
4. *Calamospora tener* (Leschik) Mädler 1964, sample LAM1, Lamas II section, Pm palynozone, Pereiros Formation, Lusitanian Basin.
5. *Playfordiaspora* sp., sample PC1, Parque de Campismo section, CG palynozone, Conraria Formation, Lusitanian Basin.
6. *Playfordiaspora* sp., sample Amorosa4(−20 cm), Amorosa section, SC palynozone, Silves Sandstones, Algarve Basin.
7. *Converrucosisporites* sp., sample AUTOB5(+2,10), International Racetrack of Algarve section, AT palynozone, Silves Sandstones, Algarve Basin.
8. *Verrucosisporites* sp., sample AUTO3, International Racetrack of Algarve section, AT palynozone, Silves Sandstones, Algarve Basin.
9. *Polypodiisporites* sp., sample LAM1, Lamas II section, Pm palynozone, Pereiros Formation, Lusitanian Basin.
10. *Porcellispora longdonensis* (Clarke) Scheuring emend. Morbey, 1975, sample LAM1, Lamas II section, Pm palynozone, Pereiros Formation, Lusitanian Basin.
11. *Porcellispora longdonensis* (Clarke) Scheuring emend. Morbey, 1975, sample CARVA1B, Carvalhais section, Coimbra Formation, Lusitanian Basin.
12. *Convolutispora* sp., sample LAMAS12, Lamas I section, Pm palynozone, Pereiros Formation, Lusitanian Basin.
13. *Anapiculatisporites* sp., sample MSGvd7, Loulé Rock Salt Mine section, CP palynozone, Silves Marl–Carbonate Evaporitic Complex, Algarve Basin.
14. *Carnisporites spiniger* (Leschik) Morbey, 1975, sample D2, Albufeira's Diapir section, Silves Marl–Carbonate Evaporitic Complex, Algarve Basin.
15. *Carnisporites* sp., sample LAM12, Lamas II section, Pm palynozone, Pereiros Formation, Lusitanian Basin.
16. *Deltoidospora* sp., sample LAM5, Lamas II section, Pm palynozone, Pereiros Formation, Lusitanian Basin.
17. *Deltoidospora* sp., sample AUTOB3, International Racetrack of Algarve section, AT palynozone, Silves Sandstones, Algarve Basin.
18. *Deltoidospora toralis* (Leschick) Lund 1977, sample MSGvd7, Loulé Rock Salt Mine section, CP palynozone, Silves Marl–Carbonate Evaporitic Complex, Algarve Basin.
19. *Nevesisporites* cf. *vallatus* Jersey & Paten 1964, sample AUTO3, International Racetrack of Algarve section, AT palynozone, Silves Sandstones, Algarve Basin.
20. *Cyathidites* sp., sample LAM1, Lamas II section, Pm palynozone, Pereiros Formation, Lusitanian Basin.
21. *Lycopodiacidites rugulatus* (Couper) Schulz 1967, sample AUTO3, International Racetrack of Algarve section, AT palynozone, Silves Sandstones, Algarve Basin.
22. *Leptolepidites argenteaeformis* (Bolkhovitina) Morbey, 1975, sample MSGvd7, Loulé Rock Salt Mine section, CP palynozone, Silves Marl–Carbonate Evaporitic Complex, Algarve Basin.
23. *Leptolepidites* sp., sample CVII-3, Castelo Viegas II section, Pm palynozone, Pereiros Formation, Lusitanian Basin.
24. *Conbaculatisporites* sp., sample AUTO3, International Racetrack of Algarve section, AT palynozone, Silves Sandstones, Algarve Basin.

relatively well preserved and consists of two genera and two species of pollen, two genera of spores, and one genus of algae. It includes the pollen *Araucariacites* sp., malformed specimens of *Classopollis* sp., *Classopollis meyerianus*, *Classopollis torosus,* and *Classopollis* sp., as well as the spores *Carnisporites* sp., and *Deltoidospora* sp.. The algae *Leiosphaeridia* sp. is also present. This palynoassemblage is extremely impoverished and dominated by *Classopollis* spp. (e.g., *Classopollis meyerianus, Classopollis torosus, Classopollis* sp. and malformed specimens of *Classopollis* sp.) and common *Araucariacites* sp.. The malformed specimens, usually in tetrads, are often characterized by one of the four grains, smaller, darker, and unornamented, indicative of reproductive stress. These malformations are associated with environmental stress conditions linked to atmospheric pollution, presence of toxic elements (e.g., mercury), enhanced UV-B radiation, which may have induced mutagenesis in terrestrial plants during the end-Triassic (Visscher et al., 2004; Foster and Afonin, 2005; Whiteside et al., 2007, 2010; Cirilli et al., 2009; Filipiak and Racki, 2010; Kürschner et al., 2013; Hochuli et al., 2017; Lindström et al., 2019). All these factors can be linked to the emplacement of the Central Atlantic Magmatic Province (CAMP), whose magmatic activity released large amounts of greenhouse gases into the atmosphere, along with other aerosols and toxic elements, such as mercury (Blackburn et al., 2013; Percival et al., 2017). Despite the absence of age-diagnostic sporomorphs preventing a definitive chronological attribution, the strong affinities with the CP palynozone and with the evaporitic facies of the same unit (Silves Marl–Carbonate Evaporitic Complex) suggest a Rhaetian–Hettangian age for this palynoassemblage.

4.1.4. Age of the Silves Group in the Algarve Basin

Based on the palynological data, the Silves Sandstones can be dated to the early Carnian at its base (*Aulisporites astigmosus – Tulesporites briscoensis* (AT) palynozone), and to the late Carnian at its top (*Samaropollenites speciosus – Camerosporites secatus* (SC) palynozone), thus spanning the early to the late Carnian. The base of The Silves Marl–Carbonate Evaporitic Complex can be ascribed to the upper Carnian (*Samaropollenites speciosus – Camerosporites secatus* (SC) palynozone), and the upper part to the Rhaetian-lowermost Hettangian (*Cerebropollenites macroverrucosus – Perinopollenites elatoides* (CP) palynozone). Notably, the Triassic-Jurassic transition occurs at the top of the Silves Marl–Carbonate Evaporitic Complex, and is recorded within the *Cerebropollenites macroverrucosus – Perinopollenites elatoides* (CP) palynozone.

In summary, the Silves Group in the Algarve Basin spans from the early Carnian to the Hettangian.

4.2. Lusitanian Basin

The three palynozones defined for the Silves Group in the Lusitanian Basin were previously proposed and discussed in Vilas-Boas et al. (2021, 2023). They are briefly summarized here to support the discussion and the correlation with the newly investigated material from the Algarve Basin (Figs. 11 and 12).

4.2.1. *Classopollis meyerianus – Granuloperculatipollis rudis (CG) palynozone*

Data and composition: This microflora was obtained from the Conraria Formation at the Alto de São João, Parque de Campismo and Sobral Cid sections. It includes a total of sixteen genera and thirteen species of pollen and four genera of spores, all moderately to well-preserved. The association is characterized by the co-occurrence of *Classopollis meyerianus, Granuloperculatipollis rudis, Patinasporites densus, Samaropollenites speciosus* and *Vallasporites ignacii.* Additional taxa include the pollen *Duplicisporites granulatus, Paracirculina quadruplicis, Praecirculina granifer,* and the spores *Camarozonosporites* sp., *Convolutispora* sp., *Kyrtomisporis* sp., and rare to common *Playfordiaspora* sp.. The assemblage further contains *Alisporites* sp., *Cycadopites* sp., *Ellipsovelatisporites* sp., *Enzonalasporites vigens, Microcachrydites doubingeri, Microcachrydites fastidioides, Monosulcites* sp., *Ovalipollis ovalis, Triadispora staplini* and *Triadispora* sp..

Age discussion: This palynozone is based on the occurrence of sporomorphs such as *Classopollis meyerianus, Enzonalasporites vigens* and *Granuloperculatipollis rudis,* with *Patinasporites densus, Samaropollenites speciosus, Vallasporites ignacii, Duplicisporites granulatus, Paracirculina quadruplicis*, and *Praecirculina granifer.* The assemblage dates from the Norian to earliest Rhaetian.

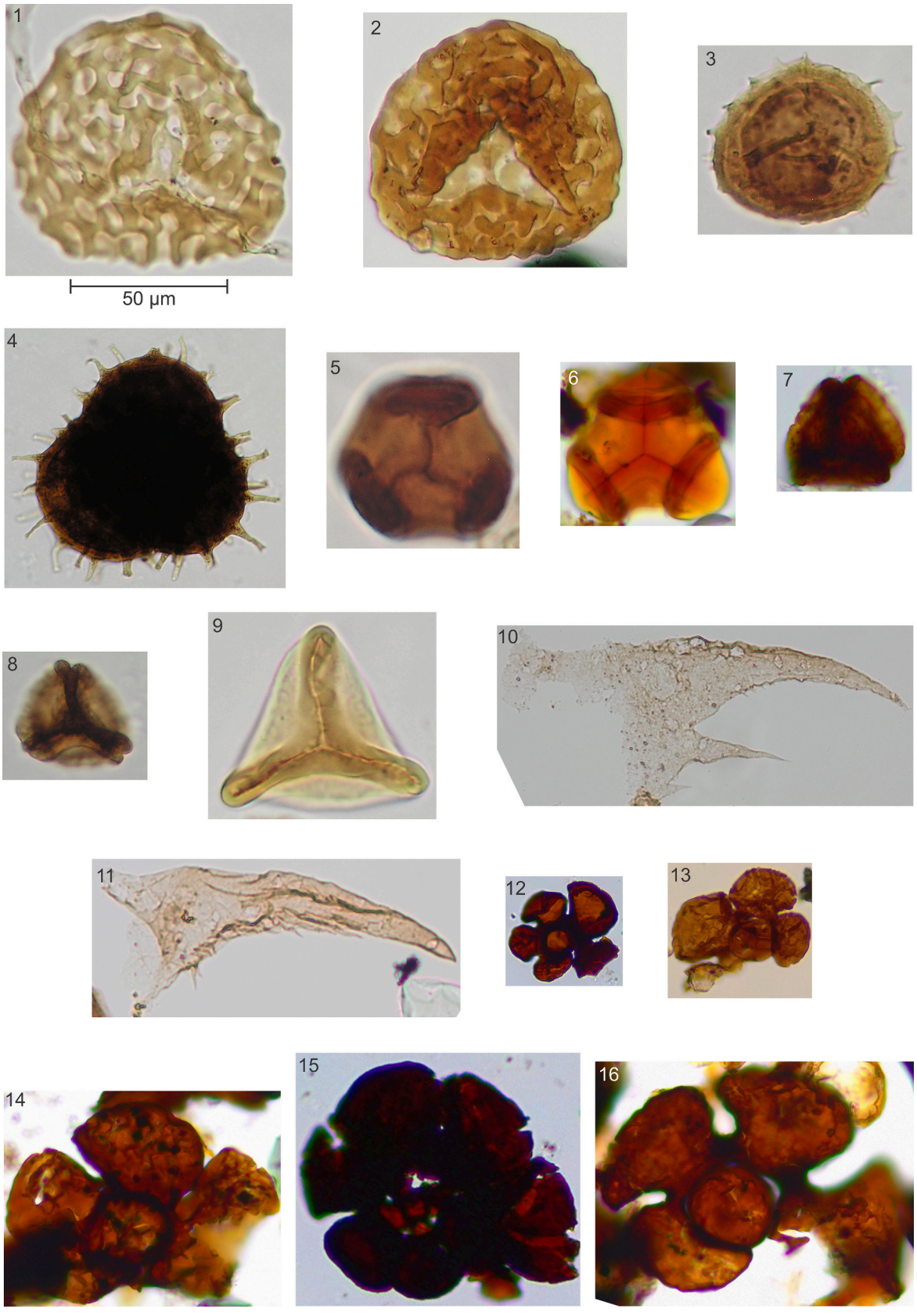

(caption on next page)

Fig. 8. Selected spores (1–9),?scolecodonts (10−11) and foraminiferal linings (12–16) from the Silves Group sections in the Algarve and Lusitanian basins, studied in this work. Species name is followed by the sample, section, unit/formation and basin.
1. *Ischyosporites variegatus* (Couper 1958) Schulz 1967, sample LAG27b, Lordemão section, IK palynozone, Pereiros Formation, Lusitanian Basin.
2. *Ischyosporites variegatus* (Couper 1958) Schulz 1967, sample CVII-3, Castelo Viegas II section, Pm palynozone, Pereiros Formation, Lusitanian Basin.
3. *Kraeuselisporites reissingeri* (Harris 1957) Morbey, 1975, sample LAM6, Lamas II section, Pm palynozone, Pereiros Formation, Lusitanian Basin.
4. *Kraeuselisporites reissingeri* (Harris 1957) Morbey, 1975, sample LAM12, Lamas II section, Pm palynozone, Pereiros Formation, Lusitanian Basin.
5. *Cibotiumspora* sp., sample LAG27b, Lordemão section, IK palynozone, Pereiros Formation, Lusitanian Basin.
6. *Cibotiumspora* sp., sample LAMAS10/11, Lamas I section, Pm palynozone, Pereiros Formation, Lusitanian Basin.
7. *Kyrtomisporis* sp., sample MSGvd6, Loulé Rock Salt Mine section, CP palynozone, Silves Marl–Carbonate Evaporitic Complex, Algarve Basin.
8. *Kyrtomisporis* sp., sample LAM12, Lamas II section, Pm palynozone, Pereiros Formation, Lusitanian Basin.
9. *Dictyophyllidites mortonii* (de Jersey) Playford & Dettman 1965, sample LAG27b, Lordemão section, IK palynozone, Pereiros Formation, Lusitanian Basin.
10.?Scolecodont or?insect, sample AM15, Amado's Beach section, SC palynozone, Silves Marl–Carbonate Evaporitic Complex, Algarve Basin.
11.?Scolecodont or?insect, sample AM15, Amado's Beach section, SC palynozone, Silves Marl–Carbonate Evaporitic Complex, Algarve Basin.
12. Foraminiferal lining, sample LAMAS13, Lamas I section, Pm palynozone, Pereiros Formation, Lusitanian Basin.
13. Foraminiferal lining, sample LAMAS8/9, Lamas I section, Pm palynozone, Pereiros Formation, Lusitanian Basin.
14. Foraminiferal lining, sample LAMAS10/11, Lamas I section, Pm palynozone, Pereiros Formation, Lusitanian Basin.
15. Foraminiferal lining, sample LAMAS13, Lamas I section, Pm palynozone, Pereiros Formation, Lusitanian Basin.
16. Foraminiferal lining, sample LAMAS10/11, Lamas I section, Pm palynozone, Pereiros Formation, Lusitanian Basin.

4.2.2. *Ischyosporites variegatus – Kraeuselisporites reissingeri (IK) palynozone*

Data and composition: The productive samples containing this assemblage were recovered from the Lordemão section, specifically from the basal part of the Pereiros Formation, which unconformably overlies the palynomorph-barren Castelo Viegas Formation. Due to the absence of palynological content in the underlying unit and the presence of an unconformity, there is insufficient evidence to establish a continuous biostratigraphy between the palynozones CG and IK. The IK palynoassemblage comprises nine genera and four species of pollen and ten genera and four species of spores, all moderately to well-preserved. It is defined by the FO of the pollen *Classopollis torosus* with the spores *Ischyosporites variegatus* and *Kraeuselisporites reissingeri.* Other components include the trilete fern spores *Dictyophyllidites mortonii* and *Todisporites major,* along with rare specimens of *Rhaetipollis germanicus,* recorded in two samples. Complete the assemblage common to abundant specimens of *Araucariacites* sp. and *Classopollis meyerianus* and rare to common *Cyathidites* sp., *Cycadopites* sp., *Ellipsovelatisporites* sp.. Additional taxa comprise *Eucommiidites* sp., *Inaperturopollenites* sp., *Monosulcites* sp., *Ovalipollis ovalis* and, the spores *Carnisporites* sp., *Cibotiumspora* sp., *Deltoidospora* sp., *Dictyophyllidites* sp., *Todisporites* sp., *Trachysporites* sp. and *Uvaesporites* sp..

Age discussion: The FO of *Ischyosporites variegatus* and *Kraeuselisporites reissingeri*, together with abundant *Classopollis* spp. and rare *Rhaetipollis germanicus* that disappears at the top of this palynozone, suggest that this palynozone represents the transitional interval across the TJB (Hillebrandt et al., 2013). The absence of key taxa (e.g., *Ricciisporites tuberculatus* and *Cerebropollenites thiergartii* Schulz, 1967 sensu lato *(= Sciadopityspollenites thiergartii* comb. nov. et emend. Gravendyck et al., 2023)) commonly recorded in palynozones that mark the Triassic–Jurassic transition, may be attributed to several plausible palaeoecological, palaeoclimatological, and taphonomical reasons (Lindström, 2016; Kürschner et al., 2014). For example, the absence of *R. tuberculatus* in the Lusitanian Basin may reflect the subtropical to tropical palaeogeographical setting of this region during the Late Triassic–Early Jurassic (Stampfli et al., 2001; Ruiz-Martínez et al., 2012; Berra and Angiolini, 2014; Scotese and Schettino, 2017). Due to a lack of palynologically productive material throughout a ~ 230 m thick stratigraphical interval, the base of the IK palynozone cannot be precisely defined in the Lusitanian Basin. Nevertheless, the available palynological data indicates that the IK palynozone spans the Rhaetian to the lowermost Hettangian, supporting the placement of the TJB within this zone, at the base of the Pereiros Formation (Vilas-Boas et al., 2021).

4.2.3. *Pinuspollenites minimus (Pm) palynozone*

Data and composition: This assemblage comes from the upper part of the Pereiros Formation, sampled at the Castelo Viegas II, Lamas I, and Lamas II sections. It comprises twelve genera and five species of pollen and twenty-two genera and eleven species of spores, all moderately to well-preserved. The assemblage is defined by the occurrence of *Classopollis meyerianus, Classopollis torosus, Perinopollenites elatoides* and *Pinuspollenites minimus* with the spores *Calamospora tener, Carnisporites spiniger, Deltoidospora hallii, Dictyophyllidites mortonii, Foveosporites foveoreticulatus, Ischyosporites variegatus, Kraeuselisporites reissingeri, Leiotriletes directus, Porcellispora longdonensis, Retitriletes austraclavatidites and Trachysporites fuscus.* Additional taxa include the pollen *Alisporites* sp., *Araucariacites* sp., *Chasmatosporites* sp., *Classopollis* sp., abnormal specimens of *Classopollis* sp., *Cycadopites* sp., *Ellipsovelatisporites* sp., *Inaperturopollenites* sp., *Monosulcites* sp., *Paracirculina* sp. and the spores *Apiculatisporis* sp., *Carnisporites* sp., *Cibotiumspora* sp., *Cingulatisporites* sp., *Converrucosisporites* sp., *Convolutispora* sp., *Cyathidites* sp., *Deltoidospora* sp., *Dictyophyllidites* sp., *Foveosporites* sp., *Ischyosporites* sp., *Kraeuselisporites* sp., *Kyrtomisporis* sp., *Leptolepidites* sp., *Polypodiisporites* sp., *Todisporites* sp., *Trachysporites* sp. and *Uvaesporites* sp.. Samples from the Lamas I section also yielded moderately preserved microforaminiferal linings.

Age discussion: This palynozone is defined by the first occurrences (FO) of *Perinopollenites elatoides* and *Pinuspollenites minimus*, along with the FO of *Calamospora tener*, *Carnisporites spiniger* and *Porcellispora longdonensis*. It is further characterized by the acme of spores, particularly *Kraeuselisporites reissingeri*. Notably the absence of *Cerebropollenites thiergartii* is observed in all the Lusitanian Basin sections (Vilas-Boas et al., 2021, 2023). *Carnisporites spiniger*, whose FO is recorded in the Anisian (Middle Triassic) and which persists steadily throughout the Late Triassic (Vigran et al., 2014; Paterson and Mangerud, 2020), is commonly present in this assemblage. The co-occurrence of *Pinuspollenites minimus, Perinopollenites elatoides* and dominant *Classopollis meyerianus* strongly supports a Hettangian age for this palynozone. This interpretation is further reinforced by the presence of *Porcellispora longdonensis,* whose FO is documented from the Hettangian in Spain (Barrón et al., 2002, 2006), the Vicentinian Alps, Italy (Clement-Westerhof et al., 1974) and Germany (Schulz and Heunisch, 2005).

The lowermost part of the Coimbra Formation was sampled to establish in terms of age the upper boundary of the Silves Group. The moderately to well-preserved assemblage contains six genera and five species of pollen and four genera and two species of spores. It comprises the pollen *Alisporites* sp., *Araucariacites* sp., *Classopollis meyerianus, Classopollis torosus, Perinopollenites elatoides* and *Pinuspollenites minimus,* with the spores *Deltoidospora* sp., *Kraeuselisporites reissingeri, Porcellispora longdonensis* and *Trachysporites* sp.

4.2.4. *Age of the Silves Group in the Lusitanian Basin*

In conclusion, the identified palynozones enable the dating of the

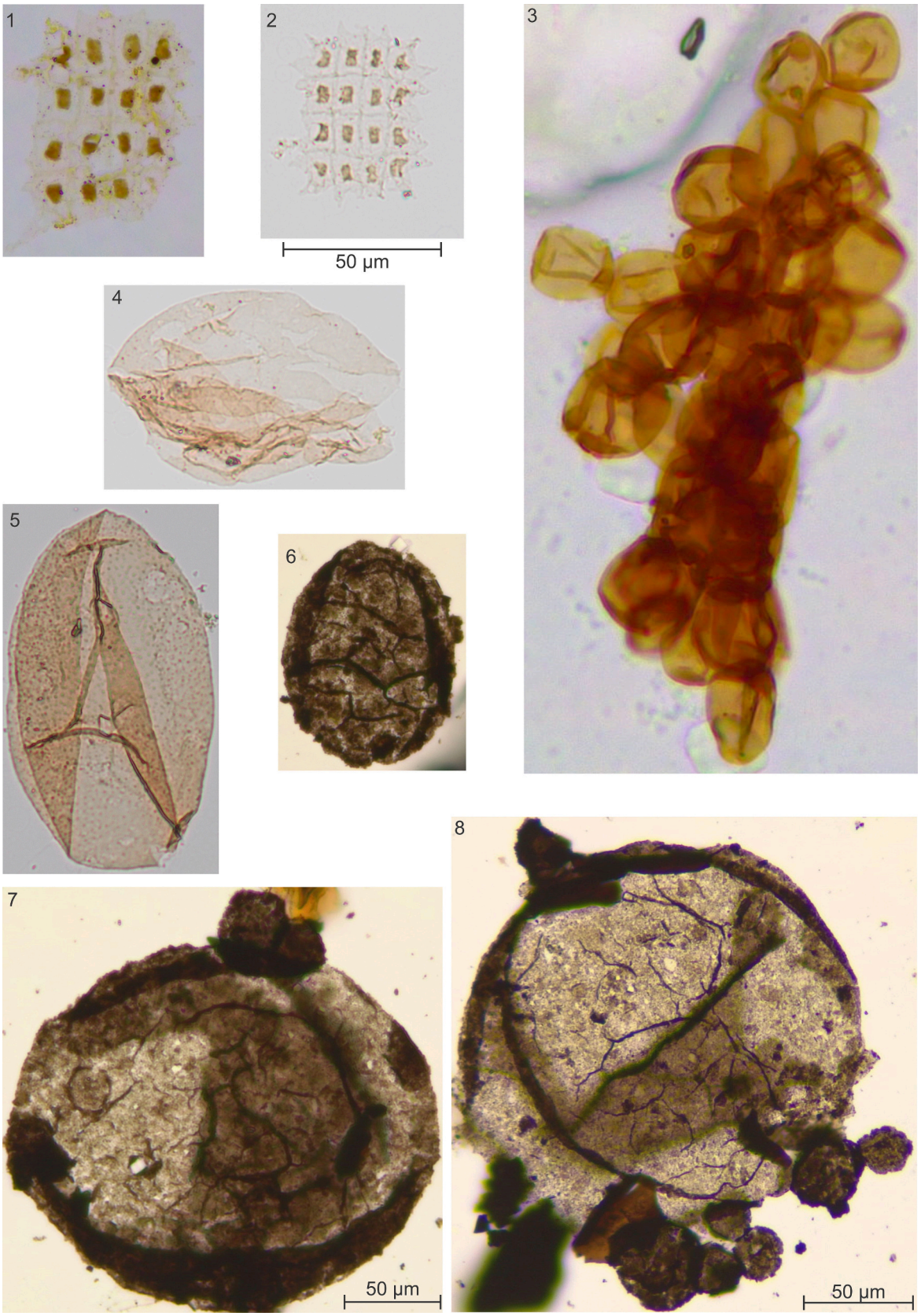

(caption on next page)

Fig. 9. Selected aquatic material from the Silves Group sections in the Algarve Basin studied in this work. Species name is followed by the sample, section, unit/formation and basin.
1. *Plaesiodictyon mosellanum* ssp. *variable* Willie 1970, sample AM15, Amado's Beach section, SC palynozone, Silves Marl–Carbonate Evaporitic Complex, Algarve Basin.
2. *Plaesiodictyon mosellanum* ssp. *variable* Willie 1970, sample AM15, Amado's Beach section, SC palynozone, Silves Marl–Carbonate Evaporitic Complex, Algarve Basin.
3. Fungal remains, sample AM15, Amado's Beach section, SC palynozone, Silves Marl–Carbonate Evaporitic Complex, Algarve Basin.
4. *Ovoidites* sp., sample AM15, Amado's Beach section, SC palynozone, Silves Marl–Carbonate Evaporitic Complex, Algarve Basin.
5. Algae sp. A, sample AM15, Amado's Beach section, SC palynozone, Silves Marl–Carbonate Evaporitic Complex, Algarve Basin.
6.?*Ourasphaira giraldae* Loron et al., 2019, sample MSG1, Loulé Rock Salt Mine section, CP palynozone, Silves Marl–Carbonate Evaporitic Complex, Algarve Basin.
7.?*Ourasphaira giraldae* Loron et al., 2019, sample MSG1, Loulé Rock Salt Mine section, CP palynozone, Silves Marl–Carbonate Evaporitic Complex, Algarve Basin.
8.?*Ourasphaira giraldae* Loron et al., 2019, sample MSG1, Loulé Rock Salt Mine section, CP palynozone, Silves Marl–Carbonate Evaporitic Complex, Algarve Basin.

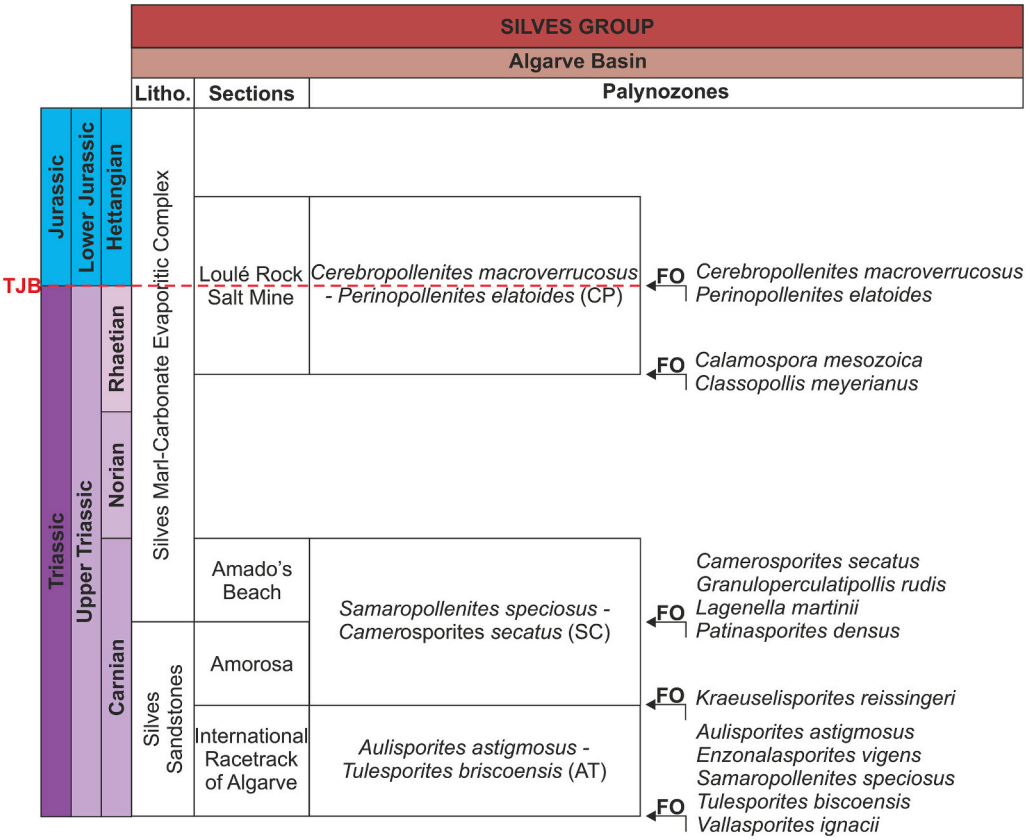

Fig. 10. Overview of the stratigraphy and the proposed new palynozones for the Silves Group in the Algarve Basin based in the first occurrence (FO) of significant palynomorphs. Litho. – Lithology. TJB – Triassic–Jurassic Boundary.

formations of the Silves Group in the Lusitanian Basin as follows.

The Conraria Formation is dated as Norian to earliest Rhaetian based on *Classopollis meyerianus-Granuloperculatipollis rudis* (CG) palynozone. For the Pereiros Formation, the lower portion is constrained to the Rhaetian–Jurassic boundary interval based on the *Ischyosporites variegatus-Kraeuselisporites reissingeri* (IK) palynozone. The middle to upper portion of the formation is dated from the early Hettangian, as indicated by the *Pinuspollenites minimus* (Pm) palynozone. Consequently, the Pereiros Formation spans the Rhaetian to the Hettangian age, with the TJB positioned at its base.

Although the Penela and Castelo Viegas formations lack palynological data due to unfavourable lithologies, their stratigraphical position between the Conraria and Pereiros formations constrains their age to the Rhaetian.

At least, the sampled basal portion of the Coimbra Formation falls within the *Pinuspollenites minimus* palynozone and can thus be assigned to the Hettangian age. In summary, the palynological data indicate that the Silves Group in the Lusitanian Basin spans from the Norian to the Hettangian.

5. The Triassic-Jurassic in Portugal: palaeoenvironmental, palaeoclimatic and palaeogeographical inferences

Although the assemblages showed unexpectedly low diversity, the material recovered from the Algarve Basin yielded valuable new information. The palynological assemblages provided refined biostratigraphical age constraints for the units of the Basin. The Silves Sandstones are assigned to the lower to upper Carnian and the Silves Marl–Carbonate Evaporitic Complex spans from the upper Carnian to Rhaetian-lower Hettangian, with the TJB identified in the upper part of this unit (Fig. 13). These data allowed us to date the Silves Group, in the Algarve Basin, from the early Carnian to early Hettangian (Fig. 13).

This age assignment, derived from palynological assemblages, is a key finding, as it constrains the onset of sedimentation throughout the Algarve Basin to the early Late Triassic.

The presence and rapid increase of the algal spores in the upper Carnian strata of the base of the Silves Marl–Carbonate Evaporitic Complex, such as *Plaesiodictyon mosellanum* ssp. *variable, Plaesiodictyon mosellanum* ssp. *bullatum, Botryococcus* spp. and *Ovoidites* sp., taxa well

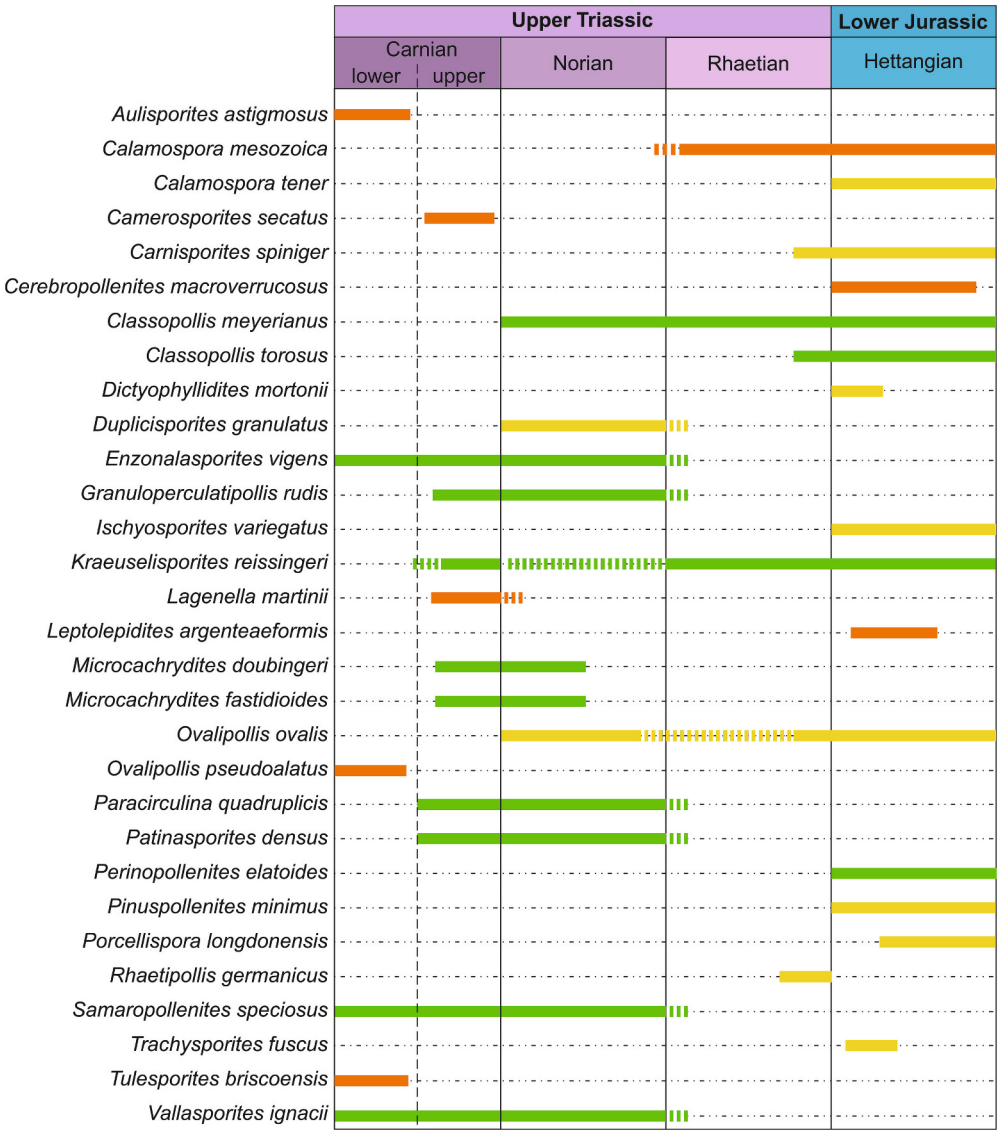

Fig. 11. Stratigraphical range chart of the most significant palynomorphs found in the Silves Group in the Algarve and Lusitanian basins. Orange line represents palynomorphs only found in the Algarve Basin. Yellow band represents palynomorphs only found in the Lusitanian Basin. Green band represents palynomorphs present in both Algarve and Lusitanian basins. The dotted ranges represent inferred occurrences in an interval with no results. (For interpretation of the references to colour in this figure legend, the reader is referred to the web version of this article.)

adapted to brackish water conditions, supports the lithological evidence indicating a palaeoenvironmental transition from continental fluvial systems (Silves Sandstones) to marginal marine settings characterized by swamps, ponds and lagoons (base of Silves Marl–Carbonate Evaporitic Complex; Fig. 14).

An attempt was made to correlate palynomorphs with the ecological affinities of their parent plants, to support palaeoclimatic and palaeoenvironmental reconstructions by inferring the likely parent plant associations and their potential ecological and climatic preferences (Table 2; Bonis and Kürschner, 2012; Césari and Colombi, 2016; Paterson et al., 2017; Lindström et al., 2017a; Li et al., 2018; Mishra et al., 2018; Baranyi et al., 2019; Tverdokhlebov et al., 2020). Based on the water requirements and adaptive strategies of the parent plants, the sporomorphs were classified into two major ecological groups: those produced by hygrophytic plants, which thrive in moist environments, and those produced by xerophytic plants, adapted to arid or seasonally dry conditions (Fig. 15; Tables 2 and 3; Bonis and Kürschner, 2012; Césari and Colombi, 2016; Paterson et al., 2017; Lindström et al., 2017a; Li et al., 2018; Mishra et al., 2018; Baranyi et al., 2019; Tverdokhlebov et al., 2020). An additional third category, the "Unknown Affinity group" includes taxa for which the botanical affinity remains uncertain (Fig. 15; Tables 2 and 3).

Analysis of the xerophytic and hygrophytic affinities of the sporomorphs from the Silves Group in the Algarve Basin reveals a persistent upward increase in taxa with xerophytic affinities, indicating a progressive shift toward warmer and drier conditions from the late Carnian to the early Hettangian (Figs. 14 and 15). This palynological trend is supported by lithological evidence showing a transition from coastal pond and lagoonal environments (at the base of the Silves Marl–Carbonate Evaporitic Complex) to a sabkha depositional setting (at the top of the Silves Marl–Carbonate Evaporitic Complex; Fig. 14).

The occurrence of malformed sporomorphs in the upper Carnian and lower Hettangian strata may reflect episodes of environmental deterioration caused by external stressors such as enhanced UVB radiation, volcanic mercury emissions, and/or atmospheric pollution (Percival et al., 2017; Lindström et al., 2019; Bos et al., 2024). Additionally, the absence of palynological material from the Norian and lower Rhaetian intervals, together with the occurrence of reworked Neoproterozoic

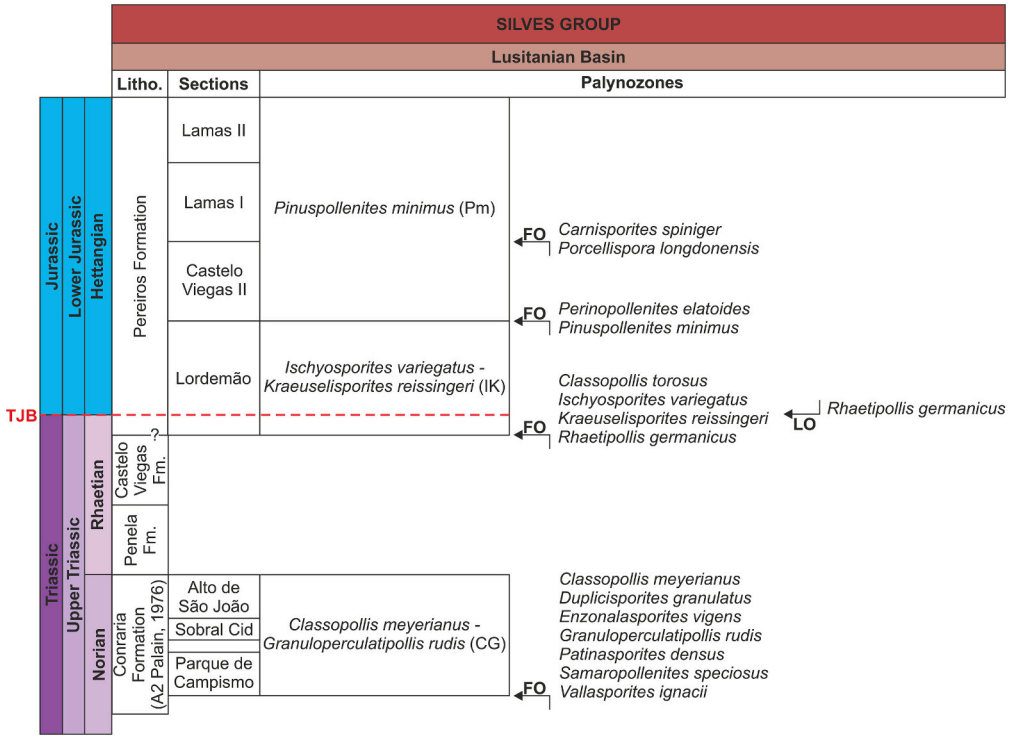

Fig. 12. Overview of the stratigraphy and the proposed new palynozones for the Silves Group in the Lusitanian Basin based in the first (FO) and last (LO) occurrence of significant palynomorphs. Litho. – Lithology. Fm. – Formation. TJB – Triassic–Jurassic Boundary.

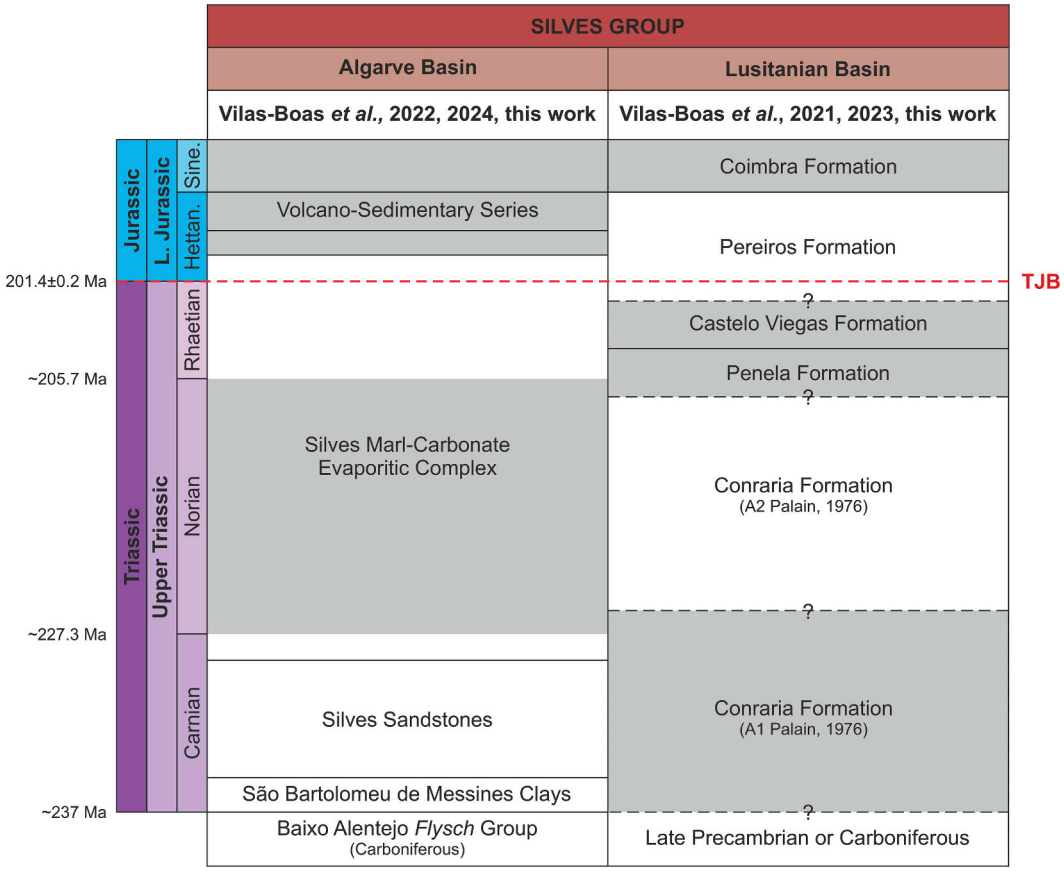

Fig. 13. New lithostratigraphical scheme proposed for the Silves Group in the Algarve and Lusitanian basins based in palynology. L. Jurassic – Lower Jurassic. Hettan. – Hettangian. Sine. – Sinemurian. TJB – Triassic–Jurassic Boundary.

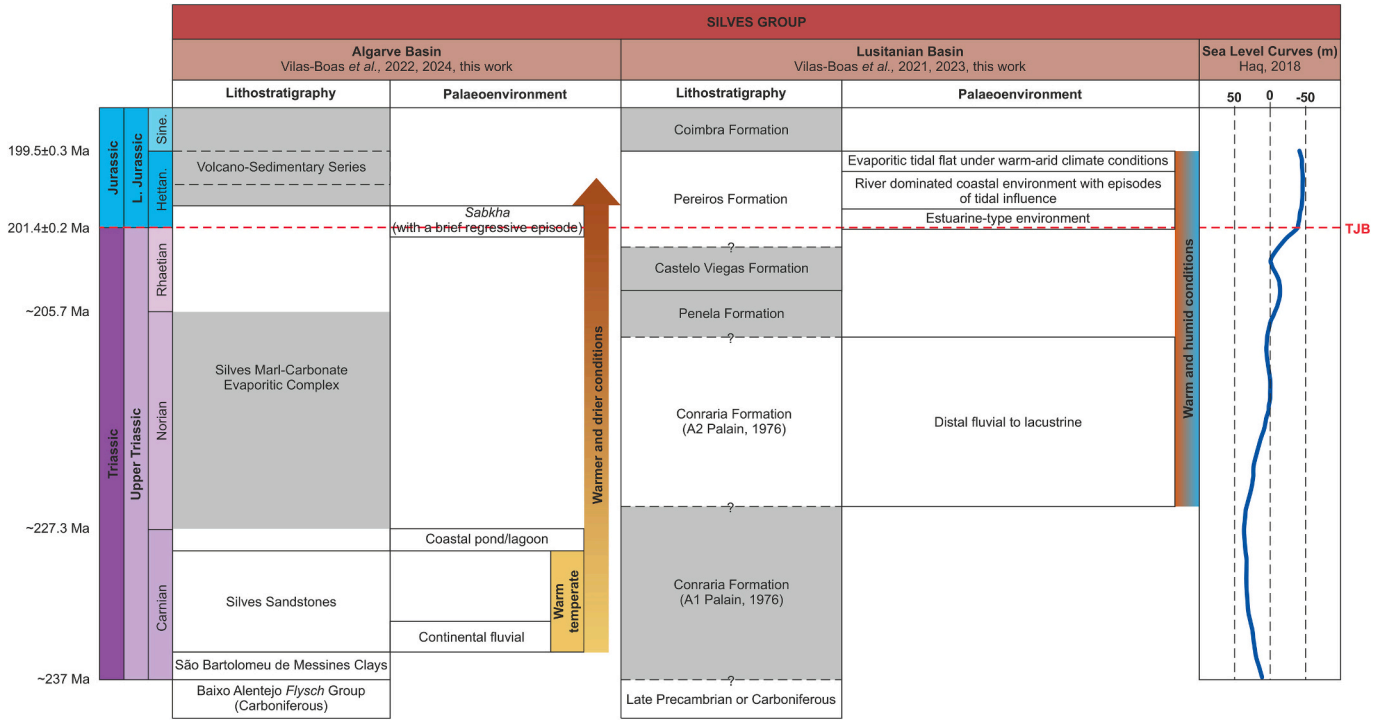

Fig. 14. Palaeoenvironmental interpretation of the Algarve and Lusitanian basin for the Upper Triassic – Lower Jurassic interval, based on palynological assemblages and their probable botanical affinities analysis. L. Jurassic – Lower Jurassic. Hettan. – Hettangian. Sine. – Sinemurian. TJB – Triassic–Jurassic Boundary.

algae (*Ourasphaira giraldae*), supports the hypothesis of a short-lived regressive phase during the Late Triassic that led to the exposure and subsequent erosion of older strata.

The co-occurrence of lower Carnian palynofloral elements with affinities with North America and Central Europe assemblages supports the inferred Late Triassic palaeogeographical position of the Iberian Peninsula (Buratti and Cirilli, 2007). The Onslow Microflora, a blend of Gondwana and European species typically found along the southwestern margins of the Tethys, includes taxa such as *Camerosporites secatus, Enzonalasporites vigens, Paracirculina quadruplicis, Paracirculina* sp., *Patinasporites densus, Samaropollenites speciosus* and *Vallasporites ignacii*. This assemblage closely resembles the Carnian microflora identified in the Algarve Basin (Cirilli and Eshet, 1991; Buratti and Cirilli, 2007). The taxonomic revision of the *Enzonalasporites* group proposed by Scibiorski et al. (2022) highlights the long-standing instability of this group. Although the present study retains the traditional nomenclature for consistency with regional zonations, future high-resolution or ultrastructural investigations may refine these assignments. Although bisaccate pollens are rare, the occurrence of *Samaropollenites speciosus*, a key taxon for palaeofloristical reconstructions, along with other typical southern elements, indicates affinity with the Onslow Microflora known from several localities of the northern hemisphere (Visscher and Krystyn, 1978; Besems, 1982; Fisher and Dunay, 1984; Adloff et al., 1985; Cirilli and Eshet, 1991; Litwin et al., 1991; Cirilli and Montanari, 1994; Góczán and Oravecz-Scheffer, 1996; Broglio Loriga et al., 1999; Roghi, 2004; Buratti and Cirilli, 2007; Traverse, 2008; Cirilli, 2010). These data offer new insights into the Carnian palaeoclimate of the Algarve Basin, suggesting that its margins experienced a warm, temperate climate, likely influenced by a monsoonal regime (Dolby and Balme, 1976; Cirilli and Eshet, 1991; Foster et al., 1994; Buratti and Cirilli, 2007; Cirilli, 2010; Césari and Colombi, 2013, 2016; Cirilli et al., 2015, 2018). The expansion of Circumpolles producers (*Cheirolepidiaceae*) toward higher latitudes during the Norian represents a key floral event linked to global climatic and palaeogeographical reorganization. The migration of *Cheirolepidiaceae* from southern Tethyan regions to higher latitudes during the Late Triassic–Early Jurassic reflects the establishment of a warm, semi-arid climate that favoured their dispersal (Cirilli, 2010; Cirilli et al., 2015, 2018). The plate-driven development of new migration pathways likely facilitated this biogeographical shift (Martini et al., 1997, 2004; Buratti and Cirilli, 2007; Cirilli, 2010). The presence of this group in both the Algarve and Lusitanian basins (Vilas-Boas et al., 2021, 2022) confirms its wide distribution and documents, at a regional scale, the reduction of microfloral provincialism leading to a more homogeneous Lower Jurassic flora.

In the Lusitanian Basin, the middle to upper part of the Conraria Formation, at the base of the Silves Group, is dated to the Norian, possibly extending into the earliest Rhaetian (Fig. 12). The TJB is located at the lower portion of the Pereiros Formation, whose palynological assemblages indicate an upper Rhaetian to early Hettangian age (Fig. 12). Precise age constraints for the intervening Penela and Castelo Viegas formations are not available, as their sandstone- and conglomerate-dominated lithologies are unsuitable for palynological analysis.

However, based on their stratigraphical position between the Conraria and Pereiros formations, these units are indirectly assigned to the Rhaetian. Overall, the Silves Group in the Lusitanian Basin spans from the Norian to the Hettangian (Fig. 13).

The earliest marine flooding episode in the Lusitanian Basin, dated as early Hettangian (e.g., Azerêdo et al., 2003; Soares et al., 2012), is documented by the presence of microforaminiferal linings at the base of the Pereiros Formation (Figs. 14 and 15). This increase in marine-derived palynomorphs and organic-walled microfossils aligns with the Early Jurassic radiation of phytoplankton in the Tethys Ocean, which has been linked to significant climatic perturbations and changes in ocean trophy during the Triassic–Jurassic transition (Van de Schootbrugge et al., 2005). Palaeoenvironmental evidence indicates that the base of this formation represents an estuarine setting, reflecting a brief marine transgression, which then evolved into coastal-tidal settings characterised by short regressive phases. The upper portion of this formation records evaporitic tidal flat conditions under arid climate (term C2 of Palain (1976), and equivalent to the Dagorda Formation). In summary, the Hettangian evolution of the Lusitanian Basin was marked

Table 2
List of sporomorphs, algae and other genera found in the Silves Group, in the Algarve and Lusitanian basins and their probable botanical affinities, ecology and possible ecological remarks.

Pollen genera	Botanical affinity	Ecology	SEGs and/or Ecological Remarks
			upper canopy, mire, wet lowland/hinterland, inhabit upland
Alisporites spp.	seed fern, Corystospermales, Peltaspermales	xerophyte	seasonally dry habitats
Araucariacites spp.	conifer, Araucariaceae	xerophyte	upper canopy, well drained, coastal
Aulisporites spp.	Cycadeoidales, Bennettitales	hygrophyte	dry lowland
Camerosporites spp.	conifer, Cheirolepidiaceae	xerophyte	hinterland
Cerebropollenites spp.	conifer, Taxodiaceae	xerophyte	upper canopy, well drained
Chasmatosporites spp.	cycad,?Cycadales	mesophyte	lowland, drier, warmer
Classopollis spp.	conifer, Cheirolepidiaceae	xerophyte	upper canopy, well drained, coastal, lowland, drier, warmer
Cycadopites spp.	gymnosperm, Cycadophyta, Ginkgoales, Peltaspermales	hygrophyte	dry lowland, warmer
Duplicisporites spp.	conifer, Cheirolepidiaceae	xerophyte	hinterland
Ellipsovelatisporites spp.	conifer	xerophyte	(?)hinterland/upland
Enzonalasporites spp.	conifer, Voltziales, Majonicaceae, Glyptolepis	xerophyte	(?)hinterland/upland
Ephedripites spp.	gymnosperm, Gnetales, Ephredraceae	xerophyte	(?)dry landscapes, (?)marginal costal plains with high degree of salt tolerance
Eucommiidites spp.	cycad, Cycadales	xerophyte	lowland, drier, warmer
Granuloperculatipollis spp.	conifer, Cheirolepidiaceae	xerophyte	upper canopy, well drained
Inaperturopollenites spp.	conifer, Taxodiaceae	xerophyte	lowland, wetter, cooler
Klausipollenites spp.	conifer,?Voltziales,?Voltziaceae	unknown	upland, canopy
Lagenella spp.	unknown	hygrophyte	river, lowland
Microcachrydites spp.	conifer, Cheirolepidiaceae, Podocarpaceae	xerophyte	upland, hinterland
Monosulcites spp.	cycad, Benettites	mesophyte	lowland, drier, warmer
Ovalipollis spp.	conifer, Voltziaceae	xerophyte	hinterland
Paracirculina spp.	conifer, Cheirolepidiaceae	xerophyte	(?)coastal
Patinasporites spp.	conifer, Voltziales, Majonicaceae	xerophyte	(?)dryland, upland, dry lowland
Perinopollenites spp.	conifer, Cupressaceae/Taxodiaceae	hygrophyte	upper canopy, mire, river
Pinuspollenites spp.	conifer, Pinaceae	mesophyte	upland
Praecirculina spp.	conifer, Cheirolepidiaceae	xerophyte	coastal
Protodiploxypinus spp.	conifer/seed fern	xerophyte	hinterland
Rhaetipollis spp.	conifer, (?)Cheirolepidiaceae	xerophyte	upland
Samaropollenites spp.	conifer, Podocarpaceae	hygrophyte	river
Triadispora spp.	conifer, Voltziaceae	xerophyte	upland, hinterland
Tulesporites spp.	unknown	unknown	unknown
Vallasporites spp.	conifer, Voltziales, Majonicaceae	xerophyte	hinterland, dry lowland, upland

Spore genera	Botanical affinity	Ecology	Ecological Remarks
Anapiculatisporites spp.	lycopsid, fern, moss?	hygrophyte	ground cover, mire, coastal, river/lowland, wet lowland
Apiculatisporis spp.	fern, Dipteridaceae	hygrophyte	lowland and river
Calamospora spp.	horsetail, Sphenophyta, Equisetopsids	hygrophyte	river, lowland, wetter, warmer, acquire wet habitat in sub-tropical and temperate regions
Carnisporites spp.	lycophyta, Filicales	hygrophyte	river, wet lowland
Camarozonosporites spp.	lycopsid	hygrophyte	river, lowland, mire
Cibotiumspora spp.	fern, pteridophyta, Cyatheaceae, Dicksoniaceae	hygrophyte	unknown
Cingulatisporites spp.	unknown	unknown	unknown
Conbaculatisporites spp.	fern, Dipteridaceae	hygrophyte	river
Converrucosisporites spp.	fern, filicopsida, Dicksoniaceae	hygrophyte	wet lowland
Convolutispora spp.	fern, pteridophyta, Schizaeaceae	hygrophyte	river
Cyathidites spp.	fern, Cyatheaceae, Dicksoniaceae, Dipteridaceae, Matoniaceae	hygrophyte	lowland, drier, warmer
Deltoidospora spp.	pteridophyta, fern, Filicales, Dicksoniaceae, Cyatheaceae, Dipteridaceae, Matoniaceae	hygrophyte	understory, mire, drier patches, dry lowland
Dictyophyllidites spp.	fern, Filicales, Dipteridaceae, Matoniaceae	hygrophyte	lowland, drier, warmer
Foveosporites spp.	pteridophyta, Selaginellales	hygrophyte	unknown
Ischyosporites spp.	pteridophyta, Schizaeaceae, Anemiaceae	hygrophyte	lowland, wetter, warmer
Kraeuselisporites spp.	lycopodiophyta, Lycopsida, Lycopodiales	hygrophyte	ground cover, mire, coastal, river
Kyrtomisporis spp.	pteridophyta, fern, Dipteridaceae	hygrophyte	river, (?)dry lowland
Leiotriletes spp.	fern, zosterophyllopsida, filicopsida, cycadopsida, ginkgoopsida	unknown	swamp, freshwater
Leptolepidites spp.	lycopsid, Filicopsida, Filicales, Pteridaceae	hygrophyte	river
Lycopodiacidites spp.	lycopsid	hygrophyte	river
Nevesisporites spp.	bryophyta, Lycopodiales	unknown	lowland and river, ground cover, mire
Playfordiaspora spp.	lycopsid	unknown	stress tolerant opportunistc plants which grow near water bodies
Polypodiisporites spp.	fern, Schizaceae, Polypodiaceae	unknown	ground cover,mire
Porcellispora spp.	bryophyte, liverwort	hygrophyte	river
Retitriletes spp.	fern, bryophyte	hygrophyte	ground cover
Todisporites spp.	fern, Osmundaceae	hygrophyte	river
Trachysporites spp.	pteridophyta, Filicales	hygrophyte	lowland and river
Uvaesporites spp.	lycopsid, Selaginellaceae	hygrophyte	river
Verrucosisporites spp.	pteridophyta, Ferns, Marattiales, Filicales especially Osmundaceae	hygrophyte	wet lowland, acquire wet habitat in sub-tropical and temperate regions

(*continued on next page*)

Table 2 (*continued*)

Pollen genera	Botanical affinity	Ecology	SEGs and/or Ecological Remarks
Algae genera	Botanical affinity		Ecological Remarks
Botryococcus spp.	chlorococcale green algae, Dictyosphaeriaceae		open water, brackish/freshwater
Leiosphaeridia spp.	Prasinophyceae		marine, swamp, lake/pond
Ovoidites spp.	Zygnemataceae, Spirogyra		shallow, stagnant, oxygen-rich fresh waters, lake margins
Plaesiodictyon mosellanum spp.	chlorococcale green algae		brackish/freshwater
Others	Botanical affinity		
Foraminiferal test linings	foraminifera (protista)		

by river-dominated sedimentation punctuated by short regressive episodes and marginal marine depositional settings.

A correlation was established between the palynomorphs found in the Lusitanian Basin and their botanical affinity, providing palaeoclimatic and palaeoenvironmental reconstructions (Fig. 15; Tables 2 and 3). Pollen dominates most of the Silves Group assemblages, except at the beginning of the Hettangian, where spores temporarily become predominant before pollen recovers its dominance. Analysis of the xerophytic versus hygrophytic affinities of the sporomorphs reveals a consistent prevalence of taxa with xerophytic adaptations, indicating persistently warm climatic conditions (Figs. 14 and 15). Nevertheless, sporomorphs with hygrophytic affinities account for approximately 22% of the assemblage across the Silves Group, suggesting that despite the overall warmth, the environment maintained significant humidity (Fig. 15, Table 3). These data indicate that the Lusitanian Basin experienced predominantly warm and humid conditions from the Norian to the Hettangian (Fig. 14). This climatic interpretation aligns with the lithofacies changes showing a distal fluvial to lacustrine setting in the Conraria Formation, transitioning into estuarine, river-dominated environments with episodic tidal influence and evaporitic tidal flats in the Pereiros Formation (Fig. 14). The environmental conditions inferred for the Hettangian succession of the Lusitanian Basin are further supported by the occurrence of microforaminiferal linings at the base of the Pereiros Formation (Fig. 15).

Future palaeogeographical and palaeoclimatic reconstructions of this sector of the Tethyan realm could greatly benefit from the Late Triassic to Early Jurassic microfloral assemblages documented in the Lusitanian Basin. Their similarities to coeval assemblages from other Tethyan basins, Western Europe, and Eastern North America suggest a persistently warm and humid climate, probably influenced by the onset of CAMP activity and intensified monsoonal circulation (Blackburn et al., 2013).

Based on the palynologically constrained ages of the Upper Triassic-Lower Jurassic successions in each basin, it can be inferred that the initial separation (i.e., the breakup) between present-day Portugal and the adjacent continental masses (North Africa and North America) began in the Algarve Basin, southern Portugal. This interpretation is supported by the occurrence of older strata in the Algarve Basin, where palynological data indicate the onset of sedimentation during the early Carnian (Vilas-Boas et al., 2022). In contrast, the oldest dated strata in the Lusitanian Basin are Norian, although this age refers to the upper part of the Conraria Formation, implying that its basal deposits may be older and potentially coeval with the base of the Silves Group in the Algarve Basin.

Comparison of the two basins with the global eustatic curve for the Triassic–Jurassic transition (Haq, 2018; Fig. 14) shows that the sedimentary record of the Algarve Basin corresponds to a regressive phase identified for this time interval. Conversely, the estuarine system developed across the TJB in the Lusitanian Basin (Fig. 14) is more consistent with a transgressive episode (Hallam, 1981, 2001; Haq et al., 1987; Haq, 2018). This apparent discrepancy may reflect the limited palynological resolution of the Lusitanian Basin, due to the scarcity of suitable samples from the older detrital units (Penela and Castelo Viegas formations), or result from localized tectonic uplift that induced a forced regression.

Despite their relatively short distance (approximately 360 km apart) (Fig. 1), the two basins exhibit notable palaeoenvironmental and palaeoclimatic differences (Fig. 14), likely related to distinct drainage networks active during the Late Triassic (Dinis et al., 2018).

Detrital zircon spectra from Silves Group sandstones indicate that the Lusitanian Basin received sediment from terranes exposed to erosion, ranging from the Mesoproterozoic to the Silurian (Dinis et al., 2018), whereas the Algarve Basin was primarily supplied by upper Neoproterozoic, Devonian, and Carboniferous source areas (Pereira et al., 2016; Dinis et al., 2018). A key distinction is the presence of Variscan-derived (Devonian–Carboniferous) sediments in the Algarve Basin, absent in the Lusitanian Basin. Furthermore, the erosion of Neoproterozoic successions may explain the occurrence, in the Algarve Basin, of reworked specimens comparable to the Proterozoic acritarch *Ourasphaira giraldae* (Loron et al., 2019). According to Dinis et al. (2018), the catchment areas that fed the two basins were separated by a topographical barrier, probably inherited from the Variscan Mountain Belt, which acted as a continental divide across the Iberian Terrane from the Late Triassic onwards.

Another major distinction is that the Silves Group sedimentary cycle in the Algarve Basin culminates with a significant volcanic phase associated with CAMP activity, whereas no equivalent magmatic phase is recorded in the Lusitanian Basin (Azerêdo et al., 2003; Verati et al., 2007; Martins et al., 2008; Kullberg et al., 2013).

These new data allow for a more refined analysis of key Late Triassic and Early Jurassic events through an integrated approach combining palynostratigraphy, palaeoecology, and palaeobiology. The palynomorph assemblages identified in this study provide critical new constraints and substantially improve the biostratigraphical, palaeoenvironmental, and palaeoclimatic framework of the Lusitanian and Algarve basins, contributing to a more comprehensive reconstruction of the Late Triassic–Early Jurassic interval within the western Tethyan realm.

6. Conclusions

The integrated palynological analysis of the Algarve and Lusitanian basins provides a new high-resolution biostratigraphical and palaeoenvironmental framework for the Late Triassic-Early Jurassic transition in Portugal.

For the Algarve Basin, three palynozones are proposed: the *Aulisporites astigmosus* – *Tulesporites briscoensis* (AT) palynozone (early Carnian), the *Samaropollenites speciosus* – *Camerosporites secatus* (SC) palynozone (late Carnian), and the *Cerebropollenites macroverrucosus* – *Perinopollenites elatoides* (CP) palynozone (latest Rhaetian- earliest Hettangian). These palynozones, for the first time, allow the dating of the entire Silves Group succession, the stratigraphical units at the base of the Algarve Basin succession, through palynostratigraphy, including a clear identification of the TJB.

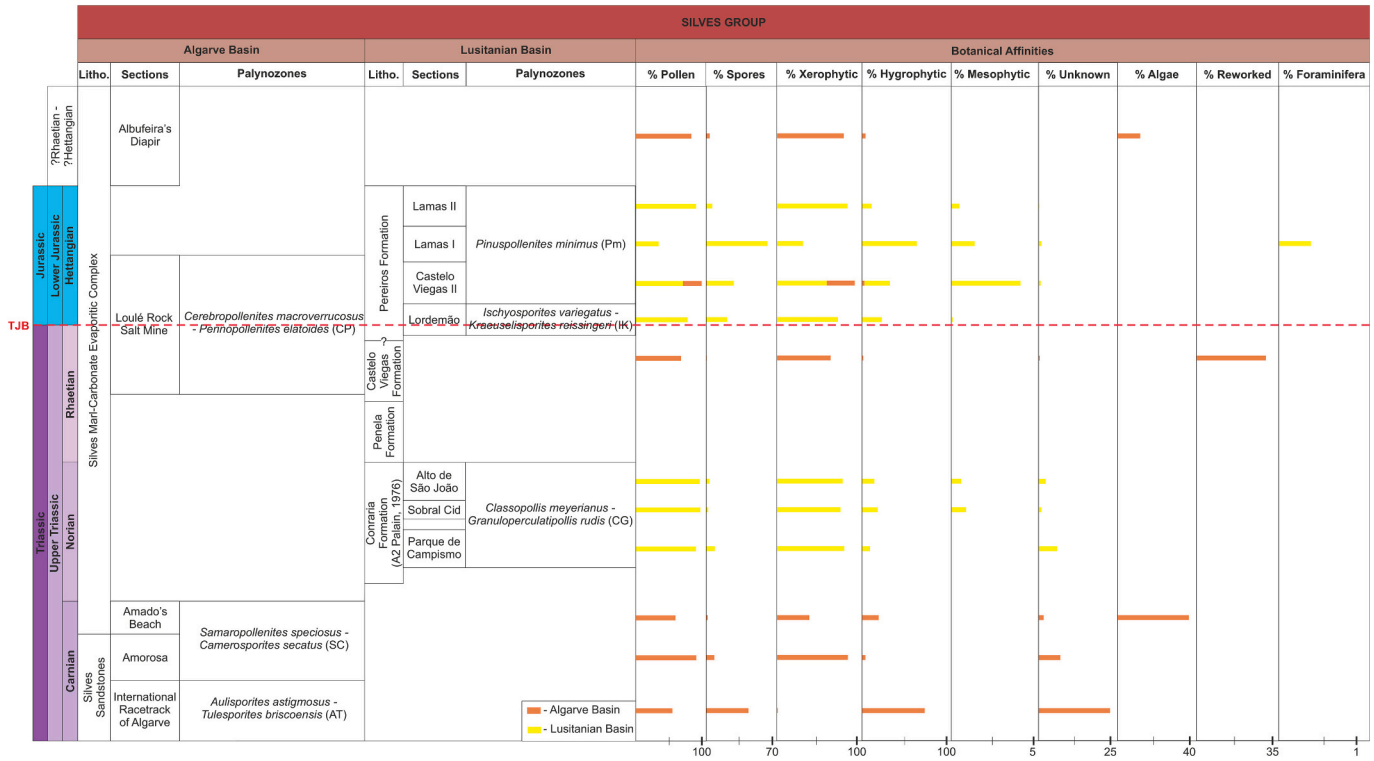

Fig. 15. Stratigraphical distribution of the palynological assemblages of the Algarve and Lusitanian basins based on their probable botanical affinities. TJB – Triassic–Jurassic Boundary. Litho. – Lithology. Fm. – Formation.

Table 3
Dataset (%) of the Silves Group palynological assemblages recovered in the studied sections in the Algarve and Lusitanian basins based on their probable botanical affinities.

		Botanical Affinity								
	Sections	% Pollen	% Spores	% Xerophytic	% Hygrophytic	% Mesophytic	% Unknown	% Algae	% Reworked	% Foraminifera
Algarve Basin	Albufeira's Diapir	84	3.8	84	3.8			12.2		
	Loulé Rock Salt Mine (upper part)	99.2	0.8	97.4	2.6					
	Loulé Rock Salt Mine (basal part)	68.6	0.1	67.5	1.1		0.1		31.3	
	Amado Beach	59.8	1.7	40.5	19.3		1.7	38.5		
	Amorosa	91.3	8.7	88.8	3.7		7.4			
	International Racetrack of Algarve	55.5	44.5	1.2	73.8		25			
Lusitanian Basin	Carvalhais	98.2	1.8	97.8	2	0.2				
	Lamas II	93.6	6.4	88.3	11	0.5	0.2			
	Lamas I	34.8	64.8	32.9	64.3	1.4	1			0.4
	Castelo Viegas II	70.5	29.5	62.8	32.3	4.2	0.7			
	Lordemão	77.6	22.4	76.6	23.3	0.1				
	Alto de São João	96.4	3.6	82.8	14.2	0.6	2.4			
	Sobral Cid	97.8	2.2	80	18.1	0.9	1			
	Parque de Campismo	90.8	9.2	84.6	9.2		6.2			

In the Lusitanian Basin, three palynozones are recognised in the Silves Group: the *Classopollis meyerianus* – *Granuloperculatipollis rudis* (CG) palynozone (Norian-earliest Rhaetian), the *Ischyosporites variegatus* – *Kraeuselisporites reissingeri* (IK) palynozone (late Rhaetian-earliest Hettangian, encompassing the TJB), and the *Pinuspollenites minimus* (Pm) palynozone (Hettangian). Collectively, these date the Silves Group succession, in the Lusitanian Basin, from the Norian to the Hettangian.

The temporal offset between the two basins confirms that the rifting associated with the breakup of Pangaea was diachronous. Sedimentation began earlier in the Algarve Basin, indicating that the initial separation between the Iberian and adjacent plates (North Africa and North America) was more advanced in southern Portugal.

Despite their proximity, the basins followed distinct evolutionary paths. The Algarve Basin transitioned from fluvial systems to restricted marginal-marine lagoons (Carnian) and eventually to sabkhas (late Rhaetian-earliest Hettangian). By contrast, the Lusitanian Basin remained a river-dominated estuarine setting, recording its earliest marine incursion via microforaminiferal linings only in the early Hettangian.

Quantitative data indicate a persistent dominance of xerophytic taxa across both basins, signalling a regional shift toward warmer, seasonally dry conditions. However, the Lusitanian Basin maintained a higher proportion of hygrophytic elements, suggesting more humid local conditions than the arid sabkhas of the Algarve Basin.

The discovery of malformed sporomorphs in both basins during the late Carnian-early Norian and across the TJB serves as a biological proxy for the environmental impact of the Central Atlantic Magmatic Province (CAMP). These malformations likely reflect mutagenesis induced by atmospheric pollution, mercury toxicity, and increased UV-B radiation.

Finally, the recovery of the Onslow Microflora and *Tulesporites briscoensis* confirms strong phytogeographical links with the western Tethyan margin and North America, while reworked Neoproterozoic algae in the Algarve Basin support the presence of an inherited Variscan topographical barrier separating the drainage networks of the two basins.

CRediT authorship contribution statement

Margarida Vilas-Boas: Writing – review & editing, Writing – original draft, Visualization, Validation, Supervision, Software, Resources, Project administration, Methodology, Investigation, Funding acquisition, Formal analysis, Data curation, Conceptualization. **Simonetta Cirilli:** Writing – review & editing, Writing – original draft, Visualization, Validation, Supervision, Resources, Project administration, Investigation, Funding acquisition, Formal analysis, Conceptualization. **Zélia Pereira:** Writing – review & editing, Writing – original draft, Visualization, Validation, Supervision, Resources, Methodology, Investigation, Funding acquisition. **Luís Vítor Duarte:** Writing – review & editing, Writing – original draft, Visualization, Validation, Supervision, Methodology, Investigation. **Paulo Fernandes:** Writing – review & editing, Writing – original draft, Visualization, Validation, Supervision, Resources, Methodology, Investigation, Funding acquisition.

Declaration of competing interest

The authors declare that they have no known competing financial interests or personal relationships that could have appeared to influence the work reported in this paper.

Acknowledgments

MVB acknowledges the Ph.D. scholarship awarded by the Fundação para a Ciência e Tecnologia (FCT) with the reference SFRH/BD/144125/2019. SC and MVB acknowledge MUR PRIN Project 2022 (cod 2022APF9M2) "Abrupt Lithofacies Variations in the stratigraphic record: proxies for environmental and climate changes - ALVIN" (P.I. S. Cirilli), the Research Funds 2021 (University of Perugia)–WP5.2, Climate changes: scientific models, technology and social impacts and the Department of Physics and Geology, University of Perugia (Funds of the Dipartimento di Eccellenza, 2023-2027 Eccellenza SUPER-C).

Appendix A. Supplementary data

Supplementary data to this article can be found online at https://doi.org/10.1016/j.palaeo.2026.113824.

Data availability

The authors confirm that all data necessary for supporting the scientific findings of this paper have been provided.

References

Adloff, M.C., Doubinger, J., Palain, C., 1974. Contribution à la palynologie du Trias et Lias Inférieur du Portugal. "grès de Silves" du Nord du tage. Comun. Serv. Geol. Port. 18, 91–144.

Adloff, M.C., Doubinger, J., Massa, D., Vachard, D., 1985. Trias de Tripolitaine (Libye). Nouvelles données biostratigraphiques et palynologiques. première partie. Rev. l'Instit. Fr. Pét 40, 723–753.

Arche, A., López-Gómez, J., 2014. The Carnian Pluvial event in Western Europe: New data from Iberia and correlation with the Western Neotethys and Eastern North America–NW Africa regions. Earth Sci. Rev. 128, 196–231. https://doi.org/10.1016/j.earscirev.2013.10.012.

Azerêdo, A.C., Duarte, L.V., Henriques, M.H., Manuppella, G., 2003. Da dinâmica continental no Triásico aos mares do Jurássico Inferior e Médio. Cadernos Geol. Portugal Inst. Geol. Min. Portugal 43.

Azerêdo, A.C., Duarte, L.V., Silva, R.L., 2014. Configuração sequencial em ciclos (2ª ordem) de fácies transgressivas-regressivas do Jurássico Inferior e Médio da Bacia Lusitânica (Portugal). Commun. Geol. 101 (1), 383–386.

Baranyi, V., Rostási, Á., Raucsik, B., Kürschner, W.M., 2019. Palynological and X-rayfluorescence (XRF) data of Carnian (Late Triassic) formations from western Hungary. Data Brief 23, 103858. https://doi.org/10.1016/j.dib.2019.103858.

Barbacka, M., Pacyna, G., Kocsis, Á.T., Jarzynka, A., Ziaja, J., Bodor, E., 2017. Changes in terrestrial floras at the Triassic-Jurassic boundary in Europe. Palaeogeogr. Palaeoclimatol. Palaeoecol. 480, 80–93. https://doi.org/10.1016/j.palaeo.2017.05.024.

Barrón, E., Gómez, J.J., Goy, A., 2002. Los materiales del tránsito Triásico–Jurásico en la región de Villaviciosa (Asturias, España). Caracterización palinológica. Geogaceta 31, 197–200.

Barrón, E., Gómez, J.J., Goy, A., Pieren, A.P., 2006. The Triassic–Jurassic boundary in Asturias (northern Spain): palynological characterisation and facies. Rev. Palaeobot. Palynol. 138 (3–4), 187–208. https://doi.org/10.1016/j.revpalbo.2006.01.002.

Berra, F., Angiolini, L., 2014. The evolution of the tethys region throughout the phanerozoic: a brief tectonic reconstruction. In: Marlow, L., Kendall, C., Yose, L. (Eds.), Petroleum Systems of the Tethyan Region. AAPG Mem., vol. 106, pp. 1–27. https://doi.org/10.1306/13431840M1063606.

Besems, R.E., 1982. Aspects of middle and late Triassic palynology. 4. On the Triassic of the External Zone of the Betic Cordilleras in the Province of Jaén Southern Spain (with a note on the presence of cretaceous palynomorphs in a presumed "Keuper"section). In: Proceedings of the Koninklijke Nederlandse Akademie, Wetenschappen, vol. 85, pp. 1–27.

Black, B.A., Karlstrom, L., Mather, T.A., 2021. The life cycle of large igneous provinces. Nat. Rev. Earth Environ. 2 (12), 840–857. https://doi.org/10.1038/s43017-021-00221-4.

Blackburn, T.J., Olsen, P.E., Bowring, S.A., McLean, N.M., Kent, D.V., Puffer, J., McHone, G., Rasbury, E.T., Et-Touhami, M., 2013. Zircon U-Pb geochronology links the end Triassic extinction with the Central Atlantic magmatic province. Sci 340 (6135), 941–945. https://doi.org/10.1126/science.1234204.

Blendinger, E., 1988. Palynostratigraphy of the late Ladinian and Carnian in the southeastern Dolomites. Rev. Palaeobot. Palynol. 53 (3–4), 329–348. https://doi.org/10.1016/0034-6667(88)90038-3.

Bonis, N.R., Kürschner, W.M., 2012. Vegetation history, diversity patterns, and climate change across the Triassic/Jurassic boundary. Paleobiology 38 (2), 240–264. https://doi.org/10.1666/09071.1.

Bonis, N.R., Ruhl, M., Kürschner, W.M., 2010. Climate change driven black shale deposition during the end-Triassic in the western Tethys. Palaeogeogr. Palaeoclimatol. Palaeoecol. 290 (1–4), 151–159. https://doi.org/10.1016/j.palaeo.2009.06.016.

Bos, R., Zheng, W., Lindström, S., Sanei, H., Waajen, I., Fendley, I.M., Mather, T.A., Wang, Y., Rohovec, J., Navrátil, T., Sluijs, A., Van de Schootbrugge, B., 2024. Climate-forced hg-remobilization associated with fern mutagenesis in the aftermath of the end-Triassic extinction. Nat. Commun. 15 (1), 3596. https://doi.org/10.1038/s41467-024-47922-0.

Broglio Loriga, C., Cirilli, S., De Zanche, V., Di Bari, D., Gianolla, P., Laghi, G.F., Lowrie, W., Manfrin, S., Mastandrea, A., Mietto, P., Muttoni, G., Neri, C., Posenato, R., Reichichi, M., Rettori, R., Roghi, G., 1999. The prati di Stuores/Stuores Wiesen section (Dolomites, Italy): a candidate global stratotype section and point for the base of the Carnian stage. Riv. Ital. Paleontol. Stratigr. 105, 37–78. https://doi.org/10.13130/2039-4942/5365.

Brusatte, S.L., Butler, R.J., Mateus, O., Steyer, J.S., 2015. A new species of metoposaurus from the late Triassic of Portugal and comments on the systematics and biogeography of metoposaurid temnospondyls. J. Vertebr. Paleontol. 35 (3), e912988. https://doi.org/10.1080/02724634.2014.912988.

Buratti, N., Cirilli, S., 2007. Microfloristic provincialism in the upper Triassic Circum-Mediterranean area and palaeogeographic implication. Geobios 40, 133–142. https://doi.org/10.1016/j.geobios.2006.06.003.

Buratti, N., Mehdi, D., Cirilli, S., Kamoun, F., Mzoughi, M., 2012. A Carnian (Julian) microflora from the Djerba Melita 1 borehole (Gulf of Gabes, South-eastern Tunisia). Micropaleontol 377–388.

Capriolo, M., Marzoli, A., Aradi, L.E., Callegaro, S., Dal Corso, J., Newton, R.J., Mills, B.J. W., Wignall, P.B., Bartoli, O., Baker, D.R., Youbi, N., Remusat, L., Spiess, R., Szabó, C., 2020. Deep CO2 in the end-Triassic Central Atlantic Magmatic Province. Nat. Commun. 11 (1), 1670. https://doi.org/10.1038/s41467-020-15325-6.

Capriolo, M., Marzoli, A., Aradi, L.E., Ackerson, M.R., Bartoli, O., Callegaro, S., Dal Corso, J., Ernesto, M., Vasconcellos, E.M.G., De Min, A., Newton, R.J., Szabó, C., 2021. Massive methane fluxing from magma–sediment interaction in the end-Triassic Central Atlantic Magmatic Province. Nat. Commun. 12 (1), 5534. https://doi.org/10.1038/s41467-021-25510-w.

Carvalho, G.S., 1950. Considerações sobre a estratigrafia das formações mais antigas da Orla Meso-Cenozóica Ocidental de Portugal. Mem. Not. Pub. Mus. Lab. Min. Geol. Univ. Coimbra 27, 17–27.

Césari, S.N., Colombi, C.E., 2013. A new Late Triassic phytogeographical scenario in westernmost Gondwana. Nat. Commun. 4 (1), 1889. https://doi.org/10.1038/ncomms2917.

Césari, S.N., Colombi, C.E., 2016. Palynology of the Late Triassic Ischigualasto Formation, Argentina: paleoecological and paleogeographic implications.

Palaeogeogr. Palaeoclimatol. Palaeoecol. 449, 365–384. https://doi.org/10.1016/j.palaeo.2016.02.023.
Choffat, P., 1903. L'Infralias et le Sinémurien du Portugal. Comun. Serv. Geol. Port. 5, 49–114.
Cirilli, S., 2010. Upper Triassic–lowermost Jurassic palynology and palynostratigraphy: a review. Geol. Soc. Lond. Spec. Publ. 334, 285–314. https://doi.org/10.1144/SP334.12.
Cirilli, S., Eshet, Y., 1991. First discovery of Samaropollenites and the Onslow Microflora in the Upper Triassic of Israel, and its phytogeographic implications. Palaeogeogr. Palaeoclimatol. Palaeoecol. 85 (3–4), 207–212. https://doi.org/10.1016/0031-0182(91)90160-S.
Cirilli, S., Montanari, L., 1994. The evaporitic Carnian succession of Bistriça River (southern Albany). Palaeopelagos 4, 107–118.
Cirilli, S., Marzoli, A., Tanner, L., Bertrand, H., Buratti, N., Jourdan, F., Bellieni, G., Kontak, D., Renne, P.R., 2009. Latest Triassic onset of the Central Atlantic magmatic province (CAMP) volcanism in the Fundy basin (Nova Scotia): new stratigraphic constraints. Earth Planet. Sci. Lett. 286 (3–4), 514–525. https://doi.org/10.1016/j.epsl.2009.07.021.
Cirilli, S., Buratti, N., Gugliotti, L., Frixa, A., 2015. Palynostratigraphy and palynofacies of the Upper Triassic Streppenosa Formation (SE Sicily, Italy) and inference on the main controlling factors in the organic rich shale deposition. Rev. Palaeobot. Palynol. 218, 67–79. https://doi.org/10.1016/j.revpalbo.2014.10.009.
Cirilli, S., Panfili, G., Buratti, N., Frixa, A., 2018. Paleoenvironmental reconstruction by means of palynofacies and lithofacies analyses: an example from the Upper Triassic subsurface succession of the Hyblean Plateau Petroleum System (SE Sicily, Italy). Rev. Palaeobot. Palynol. 253, 70–87. https://doi.org/10.1016/j.revpalbo.2018.04.003.
Clement-Westerhof, J.A., Van Der Eem, J.G.L.A., Van Erve, A.W., Klasen, J.J., Schuurman, W.M.L., Visscher, H., 1974. Aspects of Permian, Triassic and Early Jurassic palynology of western Europe - a research project. Geol. Mijnb. 53 (6), 329–341.
Dal Corso, J., Marzoli, A., Tateo, F., Jenkyns, H.C., Bertrand, H., Youbi, N., Mahmoudi, A., Font, E., Buratti, N., Cirilli, S., 2014. The dawn of CAMP volcanism and its bearing on the end-Triassic carbon cycle disruption. J. Geol. Soc. Lond. 171 (2), 153–164. https://doi.org/10.1144/jgs2013-063.
Davies, J.H.F.L., Marzoli, A., Bertrand, H., Youbi, N., Ernesto, M., Schaltegger, U., 2017. End-Triassic mass extinction started by intrusive CAMP activity. Nat. Commun. 8 (1), 15596. https://doi.org/10.1038/ncomms15596.
Deenen, M.H., Ruhl, M., Bonis, N.R., Krijgsman, W., Kürschner, W.M., Reitsma, M., Van Bergen, M.J., 2010. A new chronology for the end-Triassic mass extinction. Earth Planet. Sci. Lett. 291 (1–4), 113–125. https://doi.org/10.1016/j.epsl.2010.01.003.
Díez, J.B., 2000. Geologia y Paleobotanica de la facies Buntsandstein en la Rama Aragonesa de la Cordillera Iberica. Implicaciones bioestratigráficas en el Peritethys Occidental. Unpublished PhD Thesis. University of Zaragoza/University Pierre et Marie Curie-París-6.
Dimuccio, L.A., Duarte, L.V., Cunha, L., 2014. Facies and stratigraphic controls of the palaeokarst affecting the Lower Jurassic Coimbra Group, Western Central Portugal. In: Rocha, R.B., Pais, J., Kullberg, J.C., Finney, S. (Eds.), Strati 2013. First International Congress on Stratigraphy. At the Cutting Edge of Stratigraphy, vol. XLV. Springer Geology, pp. 787–791. https://doi.org/10.1007/978-3-319-04364-7_148.
Dimuccio, L.A., Duarte, L.V., Cunha, L., 2016. Definição litostratigráfica da sucessão calcodolomítica do Jurássico Inferior da região de Coimbra-Penela (Bacia Lusitânica, Portugal). Commun. Geol. 103 (1), 77–96.
Dinis, P.A., Fernandes, P., Jorge, R.C., Rodrigues, B., Chew, D.M., Tassinari, C.G., 2018. The transition from Pangea amalgamation to fragmentation: Constraints from detrital zircon geochronology on West Iberia paleogeography and sediment sources. Sediment. Geol. 375, 172–187. https://doi.org/10.1016/j.sedgeo.2017.09.015.
Dolby, J.H., Balme, B.E., 1976. Triassic palynology of the Carnarvon Basin, Western Australia. Rev. Palaeobot. Palynol. 22 (2), 105–168. https://doi.org/10.1016/0034-6667(76)90053-1.
Doubinger, J., Adloff, M., Palain, C., 1970. Nouvelles précisions stratigraphiques sur la série de base du Mésozoïque portugais. C. R. Acad. Sci. Paris 270, 1770–1772.
Duarte, L.V., Comas-Rengifo, M.J., Silva, R.L., Paredes, R., Goy, A., 2014. Carbon isotope stratigraphy and ammonite biochronostratigraphy across the Sinemurian-Pliensbachian boundary in the western Iberian margin. Bull. Geosci. 89 (4), 719–736. https://doi.org/10.3140/bull.geosci.1476.
Duarte, L.V., Silva, R.L., Azerêdo, A.C., Comas-Rengifo, M.J., Mendonça Filho, J.G., 2022. Shallow-water carbonates of the Coimbra Formation, Lusitanian Basin (Portugal): contributions to the integrated stratigraphic analysis of the Sinemurian sedimentary successions in the western Iberian Margin. C. R. Géosci. 354 (S3), 1–18. https://doi.org/10.5802/crgeos.144.
Dunay, R.E., Fisher, M.J., 1979. Palynology of the dockum group (Upper Triassic), Texas, USA. Rev. Palaeobot. Palynol. 28 (1), 61–92. https://doi.org/10.1016/0034-6667(79) 90025-3.
Fechner, G.G., 1989. Eine unterliassische Mikroflora aus dem Salzdiapir bei Loulé (Süd-Portugal). Berliner Geowissenschaftliche Abhandlungen. Reihe A. Geol. Paläont. 106, 37–47.
Filipiak, P., Racki, G., 2010. Proliferation of abnormal palynoflora during the end-Devonian biotic crisis. Geol. Q. 54 (1), 1–14.
Fisher, M.J., Dunay, R.E., 1981. Palynology and the Triassic/Jurassic boundary. Rev. Palaeobot. Palynol. 34 (1), 129–135. https://doi.org/10.1016/0034-6667(81)90070-1.
Fisher, M.J., Dunay, R.E., 1984. Palynology of the petrified forest member of the Chinle Formation (Upper Triassic), Arizona, USA. Pollen Spores 26 (2), 241–284.
Foster, C.B., Afonin, S.A., 2005. Abnormal pollen grains: an outcome of deteriorating atmospheric conditions around the Permian–Triassic boundary. J. Geol. Soc. 162 (4), 653–659. https://doi.org/10.1144/0016-764904-047.
Foster, C.B., Balme, B.E., Helby, R., 1994. First record of Tethyan palynomorphs from the Late Triassic of East Antarctica. AGSO J. Aust. Geol. Geophys. 15 (2), 239–246.
Frizon de Lamotte, D., Fourdan, B., Leleu, S., Leparmentier, F., de Clarens, P., 2015. Style of rifting and the stages of Pangea breakup. Tectonics 34 (5), 1009–1029. https://doi.org/10.1002/2014TC003760.
Góczán, F., Oravecz-Scheffer, A., 1996. Tuvalian sequence of the Balaton highland and the zsàmbék basin: Part II. characterization of sporomorph and foraminifer assemblages, biostratigraphic, palaeogeographic and geohistoric conclusion. Acta Geol. Hung. 39 (1), 33–101.
Gómez, J.J., Aguado, R., Azerêdo, A.C., Cortés, J.E., Duarte, L.V., O'Dogherty, L., Bordalo da Rocha, R., Sandoval, J., 2019. The Late Triassic—Middle Jurassic Passive Margin Stage. In: Quesada, C., Oliveira, J.T. (Eds.), The Geology of Iberia: A Geodynamic Approach. Vol. 3: The Alpine Cycle. Springer, Switzerland, pp. 113–167. https://doi.org/10.1007/978-3-030-11295-0_4.
Gradstein, F.M., Ogg, J.G., 2020. The chronostratigraphic scale. In: Geologic Time Scale 2020. Elsevier, pp. 21–32. https://doi.org/10.1016/B978-0-12-824360-2.00002-4.
Gravendyck, J., Coiffard, C., Bachelier, J.B., Kürschner, W., 2023. Re-evaluation of *Cerebropollenites thiergartii* Eberh. Schulz 1967 and related taxa; priority of *Sciadopityspollenites* and nomenclatural novelties. Grana 62 (1), 1–47. https://doi.org/10.1080/00173134.2022.2158688.
Guex, J., Bartolini, A., Atudorei, V., Taylor, D., 2004. High-resolution ammonite and carbon isotope stratigraphy across the Triassic–Jurassic boundary at New York Canyon (Nevada). Earth Planet. Sci. Lett. 225 (1–2), 29–41. https://doi.org/10.1016/j.epsl.2004.06.006.
Hallam, A., 1981. A revised sea-level curve for the early Jurassic. J. Geol. Soc. Lond. 138 (6), 735–743. https://doi.org/10.1144/gsjgs.138.6.0735.
Hallam, A., 2001. A review of the broad pattern of Jurassic sea-level changes and their possible causes in the light of current knowledge. Palaeogeogr. Palaeoclimatol. Palaeoecol. 167 (1–2), 23–37. https://doi.org/10.1016/S0031-0182(00)00229-7.
Hallam, A., Wignall, P.B., 1999. Mass extinctions and sea-level changes. Earth Sci. Rev. 48 (4), 217–250. https://doi.org/10.1016/S0012-8252(99)00055-0.
Haq, B.U., 2018. Triassic eustatic variations reexamined. GSA Today 28 (12), 4–9.
Haq, B.U., Hardenbol, J.A.N., Vail, P.R., 1987. Chronology of fluctuating sea levels since the Triassic. Science 235 (4793), 1156–1167. https://doi.org/10.1126/science.235.4793.1156.
Hesselbo, S.P., Robinson, S.A., Surlyk, F., Piasecki, S., 2002. Terrestrial and marine extinction at the Triassic-Jurassic boundary synchronized with major carbon-cycle perturbation: a link to initiation of massive volcanism? Geol 30 (3), 251–254. https://doi.org/10.1130/0091-7613(2002)030%3C0251:TAMEAT%3E2.0.CO;2.
Hesselbo, S.P., Robinson, S.A., Surlyk, F., 2004. Sea-level change and facies development across potential Triassic–Jurassic boundary horizons, SW Britain. J. Geol. Soc. 161 (3), 365–379. https://doi.org/10.1144/0016-764903-033.
Hillebrandt, A.V., Krystyn, L., Kürschner, W.M., Bonis, N.R., Ruhl, M., Richoz, S., Schobben, M.A.N., Urlichs, M., Bown, P.R., Kment, K., McRoberts, C.A., Simms, M., Tomāsových, A., 2013. The global stratotype sections and point (GSSP) for the base of the Jurassic System at Kuhjoch (Karwendel Mountains, Northern Calcareous Alps, Tyrol, Austria). Episodes 36 (3), 162–198. https://doi.org/10.18814/epiiugs/2013/v36i3/001.
Hiscott, R.N., Wilson, R.C., Gradstein, F.M., Pujalte, V., Garcia-Mondéjar, J., Boudreau, R.R., Wishart, H.A., 1990. Comparative stratigraphy and subsidence history of Mesozoic rift basins of North Atlantic. AAPG Bull. 74 (1), 60–76. https://doi.org/10.1306/0C9B2213-1710-11D7-8645000102C1865D.
Hochuli, P.A., Frank, S.M., 2000. Palynology (dinoflagellate cysts, spore-pollen) andstratigraphy of the Lower Carnian Raibl Group in the Eastern Swiss Alps. Eclogae Geol. Helv. 93 (3), 429–444.
Hochuli, P.A., Vigran, J.O., 2010. Climate variations in the Boreal Triassic - Inferred from palynological records from the Barents Sea. Palaeogeogr. Palaeoclimatol. Palaeoecol. 290 (1–4), 20–42. https://doi.org/10.1016/j.palaeo.2009.08.013.
Hochuli, P.A., Colin, J.P., Vigran, J.O., 1989. Triassic biostratigraphy of the Barents Sea area. In: Correlation in Hydrocarbon Exploration: Proceedings of the Conference Correlation in Hydrocarbon Exploration Organized by the Norwegian Petroleum Society and held in Bergen, Norway, 3–5 October 1988. Dordr. Springer Neth, pp. 131–153. https://doi.org/10.1007/978-94-009-1149-9_12.
Hochuli, P.A., Schneebeli-Hermann, E., Mangerud, G., Bucher, H., 2017. Evidence for atmospheric pollution across the Permian–Triassic transition. Geology 45 (12), 1123–1126. https://doi.org/10.1130/G39496.1.
Kullberg, J.C., Rocha, R.B., Soares, A.F., Rey, J., Terrinha, P., Azerêdo, A.C., Callapez, P., Duarte, L.V., Kullberg, M.C., Martins, L., Miranda, R., Alves, C., Mata, J., Madeira, J., Mateus, O., Moreira, M., Nogueira, C.R., 2013. A Bacia Lusitaniana: Estratigrafia paleogeografia e tectónica. In: Dias, R., Araújo, A., Terrinha, P., Kullberg, J.C. (Eds.), Geologia de Portugal, II. Livraria Escolar Editora, pp. 195–347.
Kürschner, W.M., Herngreen, G.W., 2010. Triassic palynology of central and northwestern Europe: A review of palynofloral diversity patterns and biostratigraphic subdivisions. Geol. Soc. Lond. Spec. Publ. 334 (1), 263–283. https://doi.org/10.1144/SP334.11.
Kürschner, W.M., Bonis, N.R., Krystyn, L., 2007. Carbon-isotope stratigraphy and palynostratigraphy of the Triassic–Jurassic transition in the Tiefengraben-section Northern Calcareous Alps (Austria). Palaeogeogr. Palaeoclimatol. Palaeoecol. 244 (1–4), 257–280. https://doi.org/10.1016/j.palaeo.2006.06.031.
Kürschner, W.M., Batenburg, S.J., Mander, L., 2013. Aberrant Classopollis pollen reveals evidence for unreduced (2n) pollen in the conifer family Cheirolepidiaceae during the Triassic–Jurassic transition. Proc. R. Soc. B Biol. Sci. 280 (1768), 20131708. https://doi.org/10.1098/rspb.2013.1708.

Kürschner, W.M., Mander, L., McElwain, J.C., 2014. A gymnosperm affinity for Ricciisporites tuberculatus Lundblad: implications for vegetation and environmental reconstructions in the Late Triassic. Palaeobiodivers. Palaeoenviron. 94 (2), 295–305. https://doi.org/10.1007/s12549-014-0163-y.

Kustatscher, E., Ash, S.R., Karasev, E., Pott, C., Vajda, V., Yu, J., McLoughlin, S., 2018. Flora of the late Triassic. In: The Late Triassic World: Earth in a Time of Transition, pp. 545–622. https://doi.org/10.1007/978-3-319-68009-5_13.

Leschik, G., 1956. II. Die Iso- und Mikrosporen. In: Krausel, R., Leschik, G. (Eds.), Die Keuperflora von Neuewelt bei Basel. Schweizerische Paldontologische Abhandlungen, 72. Memoires Suisses de Paleontologie, pp. 5–68.

Li, L., Wang, Y., Vajda, V., Liu, Z., 2018. Late Triassic ecosystem variations inferred by palynological records from Hechuan, southern Sichuan Basin, China. Geol. Mag. 155 (8), 1793–1810. https://doi.org/10.1017/S0016756817000735.

Lindström, S., 2016. Palynofloral patterns of terrestrial ecosystem change during the end-Triassic event–a review. Geol. Mag. 153 (2), 223–251. https://doi.org/10.1017/S0016756815000552.

Lindström, S., Erlström, M., Piasecki, S., Nielsen, L.H., Mathiesen, A., 2017a. Palynology and terrestrial ecosystem change of the Middle Triassic to lowermost Jurassic succession of the eastern Danish Basin. Rev. Palaeobot. Palynol. 244, 65–95. https://doi.org/10.1016/j.revpalbo.2017.04.007.

Lindström, S., Van De Schootbrugge, B., Hansen, K.H., Pedersen, G.K., Alsen, P., Thibault, N., Dybkjæra, K., Bjerrum, C.J., Nielsen, L.H., 2017b. A new correlation of Triassic–Jurassic boundary successions in NW Europe, Nevada and Peru, and the Central Atlantic Magmatic Province: a time-line for the end-Triassic mass extinction. Palaeogeogr. Palaeoclimatol. Palaeoecol. 478, 80–102. https://doi.org/10.1016/j.palaeo.2016.12.025.

Lindström, S., Sanei, H., Van De Schootbrugge, B., Pedersen, G.K., Lesher, C.E., Tegner, C., Heunisch, C., Dybkjær, K., Outridge, P.M., 2019. Volcanic mercury and mutagenesis in land plants during the end-Triassic mass extinction. Sci. Adv. 5, eaaw4018. https://doi.org/10.1126/sciadv.aaw4018.

Lindström, S., Callegaro, S., Davies, J., Tegner, C., Van de Schootbrugge, B., Pedersen, G. K., Youbi, N., Sanei, H., Marzoli, A., 2021. Tracing volcanic emissions from the Central Atlantic Magmatic Province in the sedimentary record. Earth-Sci. Rev. 212, 103444. https://doi.org/10.1016/j.earscirev.2020.103444.

Litwin, R.J., Traverse, A., Ash, S.R., 1991. Preliminary palynological zonation of the chinle formation, southwestern USA, and its correlation to the Newark supergroup (eastern USA). Rev. Palaeobot. Palynol. 68 (3–4), 269–287. https://doi.org/10.1016/0034-6667(91)90028-2.

Loron, C.C., Rainbird, R.H., Turner, E.C., Greenman, J.W., Javaux, E.J., 2019. Organic-walled microfossils from the late Mesoproterozoic to early Neoproterozoic lower Shaler Supergroup (Arctic Canada): diversity and biostratigraphic significance. Precambrian Res. 321, 349–374. https://doi.org/10.1016/j.precamres.2018.12.024.

Lucas, S.G., Tanner, L.H., Donohoo-Hurley, L.L., Geissman, J.W., Kozur, H.W., Heckert, A.B., Weems, R.E., 2011. Position of the Triassic–Jurassic boundary and timing of the end-Triassic extinctions on land: Data from the Moenave Formation on the southern Colorado Plateau, USA. Palaeogeogr. Palaeoclimatol. Palaeoecol. 302 (3–4), 194–205. https://doi.org/10.1016/j.palaeo.2011.01.009.

Manuppella, G., Marques, B., Rocha, R.B., 1988. Evolution tectono-sédimentaire du bassin de l'Algarve pendant le Jurassique. In: International Symposium on Jurassic Stratigraphy, vol. 2, pp. 1031–1046.

Martini, R., Vachard, D., Zaninetti, L., Cirilli, S., Cornée, J.J., Lathuilière, B., Villeneuve, M., 1997. Sedimentology, stratigraphy and micropaleontology of the Upper Triassic reefal series in Eastern Sulawesi (Indonesia). Palaeogeogr. Palaeoclimatol. Palaeoecol. 128 (1–4), 157–174. https://doi.org/10.1016/S0031-0182(97)81128-5.

Martini, R., Zaninetti, L., Lathuillière, B., Cirilli, S., Cornée, J.J., Villeneuve, M., 2004. Upper Triassic carbonate deposits of Seram (Indonesia): palaeogeographic and geodynamic implications. Palaeogeogr. Palaeoclimatol. Palaeoecol. 206 (1–2), 75–102. https://doi.org/10.1016/j.palaeo.2003.12.020.

Martins, L.T., Madeira, J., Youbi, N., Munhá, J., Mata, J., Kerrich, R., 2008. Rift-related magmatism of the Central Atlantic magmatic province in algarve, southern Portugal. Lithos 101 (1–2), 102–124. https://doi.org/10.1016/j.lithos.2007.07.010.

Marzoli, A., Renne, P.R., Piccirillo, E.M., Ernesto, M., Bellieni, G., De Min, A., 1999. Extensive 200-million-year-old continental flood basalts of the Central Atlantic Magmatic Province. Science 284 (5414), 616–618. https://doi.org/10.1126/science.284.5414.616.

Marzoli, A., Bertrand, H., Knight, K.B., Cirilli, S., Buratti, N., Vérati, C., Nomade, S., Renne, P.R., Youbi, N., Martini, R., Allenbach, K., Neuwerth, R., Rapaille, C., Zaninetti, L., Bellieni, G., 2004. Synchrony of the Central Atlantic magmatic province and the Triassic-Jurassic boundary climatic and biotic crisis. Geology 32 (11), 973–976. https://doi.org/10.1130/G20652.1.

Marzoli, A., Bertrand, H., Knight, K., Cirilli, S., Nomade, S., Renne, P., Vérati, C., Youbi, N., Martini, R., Bellieni, G., 2008. Comment on "Synchrony between the Central Atlantic magmatic province and the Triassic– Jurassic mass-extinction event? By Whiteside et al. (2007)". Palaeogeogr. Palaeoclimatol. Palaeoecol. 262, 189–193. https://doi.org/10.1016/j.palaeo.2008.01.016.

Marzoli, A., Jourdan, F., Puffer, J.H., Cuppone, T., Tanner, L.H., Weems, R.E., Bertrand, H., Cirilli, S., Bellieni, G., De Min, A., 2011. Timing and duration of the Central Atlantic magmatic province in the Newark and Culpeper basins, eastern USA. Lithos 122 (3–4), 175–188. https://doi.org/10.1016/j.lithos.2010.12.013.

Marzoli, A., Callegaro, S., Dal Corso, J., Davies, J.H., Chiaradia, M., Youbi, N., Bertrand, H., Reisberg, L., Merle, R., Jourdan, F., 2018. The Central Atlantic magmatic province (CAMP): a review. In: The Late Triassic World: Earth in a time of transition, pp. 91–125. https://doi.org/10.1007/978-3-319-68009-5_4.

Mateus, O., Butler, R.J., Brusatte, S.L., Whiteside, J.H., Steyer, J.S., 2014. The first phytosaur (Diapsida, Archosauriformes) from the Late Triassic of the Iberian Peninsula. J. Vertebr. Paleontol. 34 (4), 970–975. https://doi.org/10.1080/02724634.2014.840310.

Mehdi, D., Cirilli, S., Buratti, N., Kamoun, F., Trigui, A., 2009. Palynological characterisation of the Lower Carnian of the KEA5 borehole (Koudiat El Halfa Dome; Central Atlas, Tunisia). Geobios 42 (1), 63–71. https://doi.org/10.1016/j.geobios.2008.06.002.

Mietto, P., Andreetta, R., Broglio Loriga, C., Buratti, N., Cirilli, S., De Zanche, V., Furin, S., Gianolla, P., Manfrin, S., Muttoni, G., Neri, C., Nicora, A., Posenato, R., Preto, N., Rigo, M., Roghi, G., Spötl, C., 2007. A candidate of the Global Boundary Stratotype Section and Point for the base of the Carnian Stage (Upper Triassic): GSSP at the base of the canadensis Subzone (FAD of Daxatina) in the Prati di Stuores/Stuores Wiesen section (Southern Alps, NE Italy). Albertiana 36, 78–97.

Mietto, P., Mafrin, S., Preto, N., Rigo, M., Roghi, G., Furin, S., Gianolla, P., Posenati, R., Muttoni, G., Nicora, A., Buratti, N., Cirilli, S., Spötl, C., Ramezani, J., Bowring, S.A., 2012. The Global Boundary Stratotype Section and Point (GSSP) of the Carnian Stage (Late Triassic) at Prati Di Stuores/Stuores Wiesen Section (Southern Alps, NE Italy). Episodes 35 (3), 414–430.

Mishra, S., Aggarwal, N., Jha, N., 2018. Palaeoenvironmental change across the Permian-Triassic boundary inferred from palynomorph assemblages (Godavari Graben, south India). Palaeobiodivers. Palaeoenviron. 98 (2), 177–204. https://doi.org/10.1007/s12549-017-0302-3.

Morbey, S.J., 1975. The palynostratigraphy of the Rhaetian stage, Upper Triassic in the Kendelbachgraben, Austria. Palaeontogr. Abt. B 152, 1–75.

Morbey, S.J., 1978. Late Triassic and Early Jurassic subsurface palynostratigraphy in northwestern Europe. Palinology 1 (special issue), 355–368.

Müller, R.D., Seton, M., Zahirovic, S., Williams, S.E., Matthews, K.J., Wright, N.M., Shepard, G.E., Maloney, K.T., Barnett-Moore, M., Hosseinpour, M., Bower, D.J., Cannon, J., 2016. Ocean basin evolution and global-scale plate reorganization events since Pangea breakup. Annu. Rev. Earth Planet. Sci. 44 (1), 107–138. https://doi.org/10.1146/annurev-earth-060115-012211.

Nomade, S., Knight, K.B., Beutel, E., Renne, P.R., Verati, C., Féraud, G., Marzoli, A., Youbi, N., Bertrand, H., 2007. Chronology of the Central Atlantic Magmatic Province: implications for the Central Atlantic rifting processes and the Triassic–Jurassic biotic crisis. Palaeogeogr. Palaeoclimatol. Palaeoecol. 244 (1–4), 326–344. https://doi.org/10.1016/j.palaeo.2006.06.034.

Oliveira, J.T., Pereira, E., Ramalho, M.M., Antunes, M.T., Monteiro, J.H., 1992. Carta Geológica de Portugal à escala 1:500 000. Serv. Geol. Port., Lisb.

Palain, C., 1976. Une série détritique terrigène les "grès de Silves": Trias et Lias inférieur du Portugal. Mem. Serv. Geol. Port. 25, 377.

Palain, C., 1979. Connaissances stratigraphiques Sur la base du mésozoique portugais. Ciências Terra 5, 11–28.

Panfili, G., Cirilli, S., Dal Corso, J., Bertrand, H., Medina, F., Youbi, N., Marzoli, A., 2019. New biostratigraphic constraints show rapid emplacement of the Central Atlantic Magmatic Province (CAMP) during the end-Triassic mass extinction interval. Glob. Planet. Chang. 172, 60–68. https://doi.org/10.1016/j.gloplacha.2018.09.009.

Paterson, N.W., Mangerud, G., 2020. A revised palynozonation for the Middle–Upper Triassic (Anisian–Rhaetian) series of the Norwegian Arctic. Geol. Mag. 157 (10), 1568–1592. https://doi.org/10.1017/S0016756819000906.

Paterson, N.W., Mangerud, G., Mørk, A., 2017. Late Triassic (early Carnian) palynology of shallow stratigraphical core 7830/5-U-1, offshore Kong Karls Land, Norwegian Arctic. Palynology 41 (2), 230–254. https://doi.org/10.1080/01916122.2016.1163295.

Percival, L.M.E., Ruhl, M., Hesselbo, S.P., Jenkyns, H.C., Mather, T.A., Whiteside, J.H., 2017. Mercury evidence for pulsed volcanism during the end-Triassic mass extinction. Proc. Natl. Acad. Sci. 114 (30), 7929–7934. https://doi.org/10.1073/pnas.1705378114.

Pereira, M.F., Gama, C., Chichorro, M., Silva, J.B., Gutiérrez-Alonso, G., Hofmann, M., Linnemann, U., Gartner, A., 2016. Evidence for multi-cycle sedimentation and provenance constraints from detrital zircon U–Pb ages: Triassic strata of the Lusitanian basin (western Iberia). Tectonophysics 681, 318–331. https://doi.org/10.1016/j.tecto.2015.10.011.

Raup, D.M., Sepkoski, J.J., 1982. Mass extinctions in the marine fossil record. Science 215 (4539), 1501–1503. https://doi.org/10.1126/science.215.4539.1501.

Riding, J.B., Warny, S., 2008. Palynological Techniques, Second edition. Am. Assoc. Stratigraph. Palynol. Found., Dallas, Texas, p. 137.

Roghi, G., 2004. Palynological investigations in the Carnian of the Cave del Predil area (Julian Alps, NE Italy). Rev. Palaeobot. Palynol. 132 (1–2), 1–35. https://doi.org/10.1016/j.revpalbo.2004.03.001.

Ruiz-Martínez, V.C., Torsvik, T.H., van Hinsbergen, D.J.J., Gaina, C., 2012. Earth at 200 Ma: global palaeogeography refined from CAMP palaeomagnetic data. Earth Planet. Sci. Lett. 331, 67–79. https://doi.org/10.1016/j.epsl.2012.03.008.

Schaltegger, U., Guex, J., Bartolini, A., Schoene, B., Ovtcharova, M., 2008. Precise U–Pb age constraints for end-Triassic mass extinction, its correlation to volcanism and Hettangian post-extinction recovery. Earth Planet. Sci. Lett. 267 (1–2), 266–275. https://doi.org/10.1016/j.epsl.2007.11.031.

Scheuring, B.W., 1970. Palynologische und palynostratigraphische Untersuchungen des Keupers im Bölchentunnel (Solothurner Jura). Schweiz. Paläontol. Abh. 88, 2–119.

Schneebeli-Hermann, E., Looser, N., Hochuli, P.A., Furrer, H., Reisdorf, A.G., Wetzel, A., Bernasconi, S.M., 2018. Palynology of Triassic–Jurassic boundary sections in northern Switzerland. Swiss J. Geosci. 111 (1–2), 99–115. https://doi.org/10.1007/s00015-017-0286-z.

Schulz, E., 1967. Sporenpalätontologische untersuchungen rätoliassischer schichten im zentralteil des germanischen beckens. Paläontologische Abhandlungen Abteilung B 2, 541–633.

Schulz, E., Heunisch, C., 2005. Palynostratigraphische liederungsmöglichkeiten des deutschen Keupers. Stratigraphie von Deutschland. IV Keuper. Courier Forsch. Inst. Senckenberg 253, 43–49.
Schuurman, W.M., 1977. Aspects of Late Triassic Palynology. 2. Palynology of the "Grès et Schiste àAvicula contorta" and "Argiles de Levallois" (Rhaetian) of northeastern France and southern Luxemburg. Rev. Palaeobot. Palynol. 23 (3), 159–253. https://doi.org/10.1016/0034-6667(77)90007-0.
Schuurman, W.M., 1979. Aspects of Late Triassic Palynology. 3. Palynology of latest Triassic and earliest Jurassic deposits of the northern Limestone Alps in Austria and southern Germany, with special reference to a palynological characterization of the Rhaetian Stage in Europe. Rev. Palaeobot. Palynol. 27 (1), 53–75. https://doi.org/10.1016/0034-6667(79)90044-7.
Scibiorski, J., Peyrot, D., Lindström, S., Charles, A., Haig, D., Irmis, R.B., 2022. The *Enzonalasporites* group of Triassic pollen genera and species: new morphological and ultrastructural data, revised taxonomy and paleobiogeographical aspects. Rev. Palaeobot. Palynol. 306, 104744. https://doi.org/10.1016/j.revpalbo.2022.104744.
Scotese, C.R., Schettino, A., 2017. Late Permian-Early Jurassic paleogeography of western tethys and the world. In: Soto, J.I., Flinch, J.F., Tari, G. (Eds.), Permo-Triassic Salt Provinces of Europe, North Africa and the Atlantic Margins. Elsevier, pp. 57–95. https://doi.org/10.1016/B978-0-12-809417-4.00004-5.
Sêco, S.L.R., Duarte, L.V., Pereira, A.J.S.C., 2015. Utilização da espectrometria gama na caracterização das unidades da base do Jurássico Inferior do sector norte da Bacia Lusitânica (Portugal): dados preliminares. Commun. Geol. 102 (Especial I), 41–44.
Sepkoski, J.J., 1996. Patterns of Phanerozoic Extinction: a perspective from Global Data Bases. In: Walliser, O.H. (Ed.), Global Events and Event Stratigraphy in the Phanerozoic. Springer, Berlin, Heidelberg. https://doi.org/10.1007/978-3-642-79634-0_4.
Soares, A.F., Marques, J.F., Sequeira, A., 2007. Carta Geológica de Portugal Folha 19-D (Coimbra-Lousã) à escala 1:50000. Notícia Explicativa da Folha 19-D (Coimbra-Lousã). Inst. Nac. Eng. Tecnol. Inov. Lisb. 16–21.
Soares, A.F., Kullberg, J.C., Marques, J.F., da Rocha, R.B., Callapez, P.M., 2012. Tectono-sedimentary model for the evolution of the Silves Group (Triassic, Lusitanian basin, Portugal). Bull. Soc. Géol. Fr. 183 (3), 203–216. https://doi.org/10.2113/gssgfbull.183.3.203.
Stampfli, G.M., Mosar, J., Favre, P., Pillevuit, A., Vannay, J.C., 2001. Permo-Mesozoic evolution of the western Tethys realm: the Neo-Tethys East Mediterranean basin connection. Mém. Mus. Natl. Hist. Nat. Paris 186, 51–108.
Tanner, L.H., Lucas, S.G., Chapman, M.G., 2004. Assessing the record and causes of late Triassic extinctions. Earth-Sci. Rev. 65 (1–2), 103–139. https://doi.org/10.1016/S0012-8252(03)00082-5.
Tanner, L.H., Smith, D.L., Allan, A., 2007. Stomatal response of swordfern to volcanogenic CO2 and SO2 from Kilauea volcano. Geophys. Res. Lett. 34 (15). https://doi.org/10.1029/2007GL030320.
Terrinha, P., Rocha, R.B., Rey, J., Cachão, M., Moura, D., Roque, C., Martins, L., Valadares, V., Cabral, J., Azevedo, M.R., Barbero, L., Clavijo, E., Dias, R.P., Matias, H., Madeira, J., Silva, C.M., Munhá, J., Rebelo, L., Ribeiro, C., Vicente, J., Noiva, J., Youbi, N., Bensalah, M.K., 2006. A Bacia do Algarve: Estratigrafia, Paleogeografia e Tectónica. Geologia de Portugal No Contexto da Ibéria, pp. 1–138.
Terrinha, P., Rocha, R.B., Rey, J., Cachão, M., Moura, D., Roque, C., Martins, L., Valadares, V., Cabral, J., Azevedo, M.R., Barbero, L., Clavijo, E., Dias, R.P., Matias, H., Madeira, J., Silva, C.M., Munhá, J., Rebelo, L., Ribeiro, C., Noiva, J., Youbi, N., Bensalah, M.K., 2013. A Bacia do Algarve: Estratigrafia, paleogeografia e tectónica. Geol. Portugal Geol. Meso-Cenozóica Portugal II, 29–166.
Traverse, A., 2008. Paleopalynology. In: Landman, N.H., Jones, D.S. (Eds.), Topics in Geobiology, 28. Springer, Dordrecht, pp. 1–813.
Trudgill, M., Rae, J.W.B., Whiteford, R., Adloff, M., Crumpton-Banks, J., Van Mourik, M., Burke, A., Cuperus, M., Corsetti, F., Doherty, D., Gray, W., Greenop, R., Hong, W.L., Lepland, A., McIntyre, A., Neiroukh, N., Rose, C.V., Ruhl, M., Saunders, D., Siri, M. M.F.R., Steele, R.C.J., Stüeken, E.E., West, A.J., Ziegler, M., Greene, S.E., 2025. Pulses of ocean acidification at the Triassic-Jurassic boundary. Nat. Commun. 16 (1), 6471. https://doi.org/10.1038/s41467-025-61344-6.
Tverdokhlebov, V.P., Sennikov, A.G., Novikov, I.V., Ilyina, N.V., 2020. The youngest Triassic land vertebrate assemblage of Russia: composition and dating. Paleontol. J. 54 (3), 297–310. https://doi.org/10.1134/S0031030120030156.
Van de Schootbrugge, B., Bailey, T.R., Rosenthal, Y., Katz, M.E., Wright, J.D., Miller, K. G., Feist-Burkhardt, S., Falkowski, P.G., 2005. Early Jurassic climate change and the radiation of organic-walled phytoplankton in the Tethys Ocean. Paleobiology 31 (1), 73–97. https://doi.org/10.1666/0094-8373(2005)031<0073:ejccat>2.0.co;2.
Van De Schootbrugge, B., Payne, J.L., Tomasovych, A., Pross, J., Fiebig, J., Benbrahim, M., Föllmi, K.B., Quan, T.M., 2008. Carbon cycle perturbation and stabilization in the wake of the Triassic-Jurassic boundary mass-extinction event. Geochem. Geophys. Geosyst. 9 (4). https://doi.org/10.1029/2007GC001914.
Van De Schootbrugge, B., Quan, T.M., Lindström, S., Puttmann, W., Heunisch, C., Pross, J., Fiebig, J., Petschick, R., Rohling, H., Richoz, S., Rosenthal, Y., Falkowski, P. G., 2009. Floral changes across the Triassic Jurassic boundary linked to flood basalt volcanism. Nat. Geosci. 2 (8), 589–594. https://doi.org/10.1038/ngeo577.
Van der Eem, J.G.L.A., 1983. Aspects of middle and late Triassic palynology. 6. Palynological investigations in the Ladinian and lower Karnian of the Western Dolomites Italy. Rev. Palaeobot. Palynol. 39 (3–4), 189–300. https://doi.org/10.1016/0034-6667(83)90016-7.
Van Erve, A.W., 1977. Palynological investigation in the lower Jurassic of the Vicentinian Apls (Northeastern Italy). Rev. Palaeobot. Palynol. 23 (1), 1–117. https://doi.org/10.1016/0034-6667(77)90004-5.
Vaughan, A.P., 2007. Climate and geology–a Phanerozoic perspective. In: Williams, M., Haywood, A.M., Gregory, F.J., Schmidt, D.N. (Eds.), Deep-Time Perspectives on Climate Change: Marrying the Signal from Computer Models and Biological Proxies. Geol. Soc. Lond., pp. 5–59. https://doi.org/10.1144/TMS002.2
Verati, C., Rapaille, C., Féraud, G., Marzoli, A., Bertrand, H., Youbi, N., 2007. $^{40}Ar/^{39}Ar$ ages and duration of the Central Atlantic Magmatic Province volcanism in Morocco and Portugal and its relation to the Triassic-Jurassic boundary. Palaeogeogr. Palaeoclimatol. Palaeoecol. 244 (1–4), 308–325. https://doi.org/10.1016/j.palaeo.2006.06.033.
Vigran, J.O., Mangerud, G., Mørk, A., Worsley, D., Hochuli, P.A., 2014. Palynology and geology of the Triassic succession of Svalbard and the Barents Sea. Geol. Surv. Norway Spec. Pub. no. 14, 247. https://doi.org/10.5167/uzh-99116.
Vilas-Boas, M., Pereira, Z., Cirilli, S., Duarte, L.V., Fernandes, P., 2021. New data on the palynology of the Triassic–Jurassic boundary of the Silves Group, Lusitanian Basin, Portugal. Rev. Palaeobot. Palynol. 290, 104426. https://doi.org/10.1016/j.revpalbo.2021.104426.
Vilas-Boas, M., Paterson, N.W., Pereira, Z., Fernandes, P., Cirilli, S., 2022. The age of the first pulse of continental rifting associated with the breakup of Pangea in Southwest Iberia: new palynological evidence. J. Iber. Geol. 48 (2), 181–190. https://doi.org/10.1007/s41513-022-00189-0.
Vilas-Boas, M., Pereira, Z., Cirilli, S., Duarte, L.V., Sêco, S.L.R., Fernandes, P., 2023. Palynology and palynofacies studies in the lowermost Jurassic of the Lusitanian Basin (Pereiros Formation of the Silves Group), Portugal: evidence of the first transgressive episode. Acta Palaeobot. 63 (2), 129–150. https://doi.org/10.35535/acpa-2023-0008.
Vilas-Boas, M., Pereira, Z., Cirilli, S., Fernandes, P., 2024. New Insights on the Upper Triassic Silves Group in Algarve Basin, Portugal: Palynological, paleophytogeography and paleoclimatology advances. Geobios 86, 49–64. https://doi.org/10.1016/j.geobios.2024.08.001.
Visscher, H., Brugman, W.A., 1981. Ranges of selected palynomorphs in the Alpine Triassic of Europe. Rev. Palaeobot. Palynol. 34 (1), 115–128. https://doi.org/10.1016/0034-6667(81)90069-5.
Visscher, H., Krystyn, L., 1978. Aspects of Late Triassic palynology. 4. A palynological assemblage from ammonoid-controlled Late Karnian (Tuvalian) sediments of Sicily. Rev. Palaeobot. Palynol. 26 (1–4), 93–112. https://doi.org/10.1016/0034-6667(78)90007-6.
Visscher, H., Schuurman, W.M.L., Van Erve, A.W., 1980. Aspects of a palynological characterization of Late Triassic and Early Jurassic 'Standard' units of chronostratigraphical classification in Europe. Proc. IV Int. Palynol. Conf. Lucknow 2, 281–287.
Visscher, H., Looy, C.V., Collinson, M.E., Brinkhuis, H., Konijnenburg-van Cittert, J.H.A., Kürschner, W.M., Sephton, M.A., 2004. Environmental mutagenesis during the end-Permian ecological crisis. Proc. Natl. Acad. Sci. 101 (35), 12952–12956. https://doi.org/10.1073/pnas.0404472101.
Warrington, G., 2002. Triassic spores and pollen. In: Jansonius, J., Mcgregor, D.C. (Eds.), Palynology: Principles and Applications, 2nd edition 2. Am. Assoc. Stratigr. Palynol. Found, pp. 755–766.
Whiteside, J.H., Olsen, P.E., Kent, D.V., Fowell, S.J., Et-Touhami, M., 2007. Synchrony between the Central Atlantic magmatic province and the Triassic–Jurassic mass-extinction event? Palaeogeogr. Palaeoclimatol. Palaeoecol. 244 (1–4), 345–367. https://doi.org/10.1016/j.palaeo.2006.06.035.
Whiteside, J.H., Olsen, P.E., Eglinton, T., Brookfield, M.E., Sambrotto, R.N., 2010. Compound-specific carbon isotopes from earth's largest flood basalt eruptions directly linked to the end-Triassic mass extinction. Proc. Natl. Acad. Sci. 107 (15), 6721–6725. https://doi.org/10.1073/pnas.1001706107.
Wilson, R.C.L., 1975. Atlantic opening and Mesozoic continental margin basins of Iberia. Earth Planet. Sci. Lett. 25 (1), 33–43. https://doi.org/10.1016/0012-821X(75)90207-1.
Wilson, R.C.L., 1988. Mesozoic development of the Lusitanian basin, Portugal. Rev. Soc. Geol. Esp. 1 (3), 393–407.
Wilson, M., Guiraud, R., Moreau, C., Bellion, Y.C., 1998. Late Permian to recent magmatic activity on the African-Arabian margin of Tethys. In: Macgregor, D.S., Moody, R.T.J., Clark-Lowes, D.D. (Eds.), Petroleum geology of North Africa, vol. 132. Geol. Soc., Lond., Spec. Pub, pp. 231–263. https://doi.org/10.1144/GSL.SP.1998.132.01.14.
Wood, G.D., Gabriel, A.M., Lawson, J.E., 1996. Palynological techniques processing and microscopy. In: Jansonius, J., McGregor, D.C. (Eds.), Palynology: Principles and applications, 1. Am. Assoc. Stratigr. Palynol. Found, pp. 29–50.